A vibrotactile transducer and its applications in the study of perception

Hsin-Yun Yao

Department of Electrical & Computer Engineering
McGill University
Montreal, Canada

January 2010

A thesis submitted to McGill University in partial fulfillment of the requirements for the degree of Doctor of Philosophy.

2010/01/18

Abstract

Vibrotactile signals are ubiquitous in everyday life, occurring both when manipulating objects and operating power tools. To bring haptics to ambient systems (defined as being embedded in everyday objects), the vibrotactile channel presents itself as a perceptually and energetically efficient method of conveying haptic information.

Mobile phones are by far the most popular haptic-enabled devices. Yet, they are often equipped with common vibration motors of narrow-bandwidth capability. A voice-coil vibrotactile transducer design has been demonstrated to be high-bandwidth and capable of functioning under the same *enclosure-vibration* paradigm. The transducer was modeled by converting its mechanical free-body diagram into equivalent electrical circuits. The experimentally obtained transfer function was combined with the function established theoretically to obtain the impedance expression for each parameter.

Using the aforementioned actuator, mock cellphones were made for vibrotactile perception experiments. Employing pulsed vibration signals to combat adaptation effects, experiments were performed to study the effect of weight and underlying vibration frequency on perceived strength. Results show that for the same measured acceleration on the device, a heavier box is perceived to vibrate with greater strength. Furthermore, signals with higher underlying frequency are perceived to be weaker for the same measured acceleration. The results obtained from ungrounded, vibrating objects are consistent with previous studies using grounded devices. The findings suggest the need for a systematic correction rule that assists cellphone designers in how to modify the device's vibratory characteristics according to its weight and the operating frequency.

An ambient haptic device is implemented to synthesize haptic cues resulting from an object rolling down and impacting the inside wall of a tubular cavity. When an object rolls or slides, a variety of cues become available for the estimation of its location inside the cavity. These cues are related to the dynamics of an object subjected to the laws of physics such as gravity and friction. Perception experiments were conducted, in which participants attempted to discriminate among three virtual tubes of different lengths after making the virtual ball roll down. The results support the hypothesis that the subjects mastered the laws related to the dynamics of objects under the influence of gravity and used them to perceive the length of the invisible cavities.

Résumé

Les signaux vibrotactiles sont omniprésents dans la vie quotidienne. Ils se manifestent soit quand on manipule les objets soit lorsque l'on touche des machines. Afin de donner aux "systèmes ambiants" la possibilité de communiquer aux utilisateurs par l'haptique, les signaux vibrotactiles s'avèrent être un moyen efficace, tant au point de vue de leur perception que de la consommation énergétique.

Les téléphones portables sont, de loin, les appareils ayant des capacités haptiques les plus communs. Ils sont munis de moteurs vibrants ayant une bande passante limitée. Nous avons réalisé un transducteur vibrotactile à large bande passante et qui permet de faire vibrer la boite entière, comme dans un téléphone portable. Ce transducteur a été modélisé du point de vue de l'électromécanique, puis transformé en circuits électriques équivalents pour en faciliter l'analyse. La fonction de transfert a été obtenue expérimentalement, par puis comparée à la fonction obtenue théoriquement afin d'obtenir l'impédance de chaque composant du transducteur.

Ces transducteurs ont été utilisés dans la fabrication d'appareils pour l'étude de la perception. Une série d'expériences a été menée afin étudier l'effet du poids et de la fréquence de vibration sur la perception vibrotactile. Les résultats démontrent que pour une même accélération, on perçoit les vibrations comme étant plus fortes s'il s'agit d'un objet plus lourd. D'autre part, on les perçoit comme étant plus faibles si elles sont d'une fréquence plus élevée. Ces résultats correspondent à peu près à ceux trouvés avec des appareils fixés au sol. Par conséquent, il serait souhaitable d'avoir des règles de correction des caractéristiques des vibrations d'un appareil mobile en fonction de son poids et la fréquence de stimulation.

Un dispositif de simulation haptique a également été construit pour simuler les sensations haptiques résultantent d'un objet qui roule ou glisse au long d'une cavité tubulaire et qui heurte des paroies internes. Lorsqu'un objet roule ou glisse, plusieurs types d'indices haptiques sont disponibles et informent sur la position de l'objet. Ces indices sont liés à la dynamique de l'objet soumis aux lois du mouvement qui résulte de la gravité et de la friction. Une expérience de perception a été effectuée, où les participants faisaient rouler la balle virtuelle et tentaient d'estimer la distance parcourue. Les résultats supportent l'hypothèse que l'on maîtrise les invariants liés à la dynamique d'un objet se déplaceant

sous l'influence de la gravité, et qu'on est capable de les utiliser pour percevoir la taille de cavités invisibles.

Contributions of Authors

This is a manuscript-based thesis. As an alternative to the traditional thesis format, this thesis consists of a collection of papers, as described below.

Chapter 3 includes the manuscript entitled *Design and Analysis of A Recoil-Type Vibrotactile Transducer* by Hsin-Yun Yao and Vincent Hayward is to be submitted to the *Journal of the Acoustical Society of America*. The author of this thesis, the primary contributor, was responsible for the design, fabrication, data collection and analysis of the device, as well as the preparation of the manuscript draft. Dr. Vincent Hayward contributed to guiding and supervising the project, as well as writing the introductory section, editing and proofreading the manuscript.

Chapter 4 includes the manuscript entitled *The Effect of Weight on the Perception of Vibrotactile Intensity with Handheld Devices* by Hsin-Yun Yao, Vincent Hayward, Manuel Cruz and Danny Grant, appeared in the *Proceedings of Second Joint EuroHaptics Conference, and Symposium on Haptic Interfaces for Virtual Environment and Teleoperator Systems, 2007*. The author of this thesis, the primary contributor, was responsible for the design, execution and analysis of the experiments and the preparation of the manuscript. Dr. Vincent Hayward contributed to the reviewing and proofreading the manuscript. Dr. Manuel Cruz and Dr. Danny Grant were responsible for initializing the study and assisting the experiments design.

Chapter 5 comprises the manuscript entitled *Perceived Vibration Strength in Mobile Devices: the Effect of Weight and Frequency* by Hsin-Yun Yao, Danny Grant and Manuel Cruz was submitted and accepted in the *IEEE Transactions of Haptics* in July 2009. As the primary contributor, the author of this thesis was responsible for the design, execution and analysis of the experiments and the preparation of the manuscript. Dr. Manuel Cruz contributed to assisting the experiment design, and Dr. Danny Grant was responsible for providing feedback on the experiment design and editing and proofreading the manuscript.

Chapter 6 contains the article entitled *An Experiment on Length Perception with a Virtual Rolling Stone* by Hsin-Yun Yao and Vincent Hayward was published in the *Proceedings of EuroHaptics Conference, 2006*. The author of this thesis was responsible for the design and fabrication of the haptic device, execution and analysis of experiments, and the preparation of the manuscript. Dr. Vincent Hayward contributed in initializing

the study, providing support for the theory, writing the introductory section, editing and proofreading.

Acknowledgments

First, I would like to thank my supervisor Vincent Hayward for his encouragement, guidance and constructive criticism throughout my graduate studies, which have undoubtedly made me a better scientist and engineer. I especially appreciate his understanding about my family situation, which at times prevented me from giving my best.

I would like to thank my collaborators, Danny Grant and Manuel Cruz, for giving me the opportunity to work on a topic of immediate importance for the industry and supporting me during the study. I am thankful for Ilja Frisson and Mounia Ziat for help in psychology and statistics, as well as current and former colleagues from the Haptics Lab: Gianni Champion, Hanifa Dostmohamed, Andrew Gosline, Vincent Levesque, Jerome Pasquero, Akihiro Sato and Qi Wang.

I am most appreciative to my daughters, Eliane and Livia, for bringing joy and inspiration to my life, and "forcing" me to be efficient and organized in my work. I thank my immediate and extended family for their kindness, encouragement and free (yet top-quality) daycare services for my children.

Finally, I would like to express my gratitude toward my husband, Jean-Samuel, for his interests in my research, his unconditional support since the beginning and help in machining prototypes, assembling circuits, proofreading manuscript, making dinner and caring for the children when I couldn't. I'm forever grateful.

Contents

List of Figures

List of Tables

Chapter 1

Introduction

Ambient systems, in human-computer interaction, are systems that employ technologies in a way that they become an integral part of the user's environment. The boundary between human and machine is overcome by making the interaction natural and intuitive. To reach this goal, human-machine interfaces should communicate using several sensing and actuating channels simultaneously, as that is how we naturally interact with our environment.

Traditionally, computer devices communicate with users by obtaining input through touch and displaying output through vision or sound. By nature, the visual channel plays the primary role of displaying information from the device to the user; yet, it cannot take input from the user (except through eye movements). The most common method of gathering the user's input is through haptic means by buttons or keypad. This haptic channel, however, also has the property of communicating in the direction *back* to the user, a communication path not yet extensively explored.

Cellphones or PDAs are by far the most commonly used haptic devices. They use vibrotactile signals to communicate discretely to the owner when receiving a call or a message. The choice of vibration signal is far from random: it is an energetically and perceptually efficient way to transmit haptic information. The common vibration motor found in mobile devices is a simple DC motor with an off-centered mass, which is very economically efficient as well. However, because of its narrow bandwidth, it can only produce vibrations within a limited range of frequencies. It often works by pulses to save power and avoid fatigue. Some more sophisticated devices can deliver programmable pulsing schemes. Regardless, these vibration signals are light-years away from our rich, every day tactile experience. A comparison would be playing piano using only one note,

versus using both hands on the complete keyboard; the latter can convey more information and provide a more appealing auditory experience.

The limited haptic capability in common mobile devices is most importantly due to the narrow bandwidth of vibration motors. In order to enhance it, the logical first step would be improving the bandwidth of the actuator. This upgraded actuator would provide a better way to enrich the information transfer capability. Secondly, one common practice in the industry is linearly linking acceleration to perceived vibration strength. Yet, our perception doesn't always work in such a straightforward fashion. In fact, the above association is true for a small frequency range, and only when all other conditions are equal. In a real-life situation, many other factors, such as the device properties and contact area, are found to interfere with our strength perception.

There is undeniably a rich literature based on vibrotactile perception. However, few studies target specifically mobile devices. There are questions yet to be answered. For instance, how does the vibrotactile perception on mobile, ungrounded devices differ from that on grounded devices studied in the past? Does the vibration in pulses and short bursts used mostly and exclusively in mobile devices produce a different perceptual outcome than continuous signals? Answering these questions will not only satisfy curious minds, but also give a validated guideline to cellphone designers on ways to improve the haptic capability of the devices.

Industry applications, such as cellphones, are only a small part of what the research in haptics is all about. For many, the ultimate goal of a haptic device is to be able to recreate real-world haptic experiences. Such a device, even an imperfect one, could serve as a tool to further uncover the mystery of how the human mind and perception work, which, in turn, would help improve haptic devices.

Objectives

This doctoral study attempts to tackle three different aspects of ambient haptic systems: first, to find a better actuating technology; second, to probe further into vibrotactile perception under specific conditions; third, to contribute to a better understanding of human perception in general.

More specifically, this thesis consists of three main objectives: first, to design and build a vibration motor with better controllability and wider bandwidth; second, with an

apparatus equipped with the actuator, to carry out experiments to better understand how the device weight and signal frequency affect the vibrotactile perception on mobile devices; finally, to build an ambient haptic system simulating real-life events realistically in order to gain insights about how our central nervous system relates the received haptic stimulus to its knowledge of laws of motion.

Thesis Outline

This thesis is organized in the following way. After this introductory chapter, **Chapter 2** is a review of literature covering the different aspects of vibrotactile devices and signals, as required in a manuscript-based thesis. The basic and most common electromagnetic vibration-producing motors are surveyed with brief descriptions of their operating principles and main applications. A review of existing vibrotactile haptic devices is then presented, and particular attention is paid to their actuating systems. These devices were separated into two categories: those providing local, direct stimulation and those providing enclosure stimulation. The next focus of the review is vibrotactile perception and how different perceptual quantities are related to the signal's physical characteristics, followed by a brief survey of where vibrations arise in our daily life. The final section of the chapter is a brief overview of the theory of internal models regarding the laws of physics, especially gravity.

Chapter 3 presents a voice-coil vibrotactile transducer named the *Haptuator*. Designed to generate enclosure vibration as common vibration motors, it has a wider bandwidth capability. The operating principle of the actuator is first discussed, followed by the mechanical free body diagram and its equivalent combined electrical circuitry. The transfer function of the system is first obtained experimentally, and then matched to the theoretical expression derived from the circuitry analysis. Using the final model of the actuator, the article performed analysis for each parameter to see how varying their values may change the acceleration outcome.

Chapter 4 and 5 describes a series of experiments on vibrotactile perception on mobile devices. Using the*Haptuator*, mock cellphones are made and several experiments on mobile devices are carried out to study their vibrotactile perception. Included in Chapter 4 is a short report of a pilot experiment on how the device weight affects the perceived vibration strength. In Chapter 5, a follow-up experiment on the effect of weight is detailed, this time with more participants and a few minor changes in the experimental protocol and setup.

The results confirmed the findings from the previous experiment. A second experiment on the effect of underlying frequency on perceived vibration strength was also conducted. The findings are consistent with past studies on continuous, grounded vibrotactile perception.

Chapter 6 presents a use of the actuator in an ambient haptic system, as well as an experiment on how the laws of physics in movements are perceived when only the tactile information is available. Embedded inside a fiberglass tube of 1.6 cm diameter, the Haptuator is made to simulate the haptic signal produced by a ball rolling down the tube. This simulation is realistic enough to make most people believe there is a real ball rolling inside the device. A perception study was designed to see if people could estimate the traveled length of a rolling ball based solely on haptic cues. Participants had to tilt the tube and let the virtual ball roll down, then make a decision regarding its traveled distance. To probe further, the haptic cues were separated into the rolling, the impact, and the bouncing cues. Using the simulation, the cues were displayed either separately or combined in order to examine individually how each contributes to our judgment.

Chapter 7 is comprised of a summary and conclusive remarks, as well as potential future work.

Chapter 2

Literature Review

Tactile sensations are created by stimulation of mechanoreceptors beneath the surface of the skin, activated when mechanical force is applied to the skin. The mechanical force can be produced using rotating motors, DC motors, piezoelectrical motors, shape memory alloy elements, or any mechanism that can move the skin. Between the mechanical force and the mechanoreceptors lies the haptic interface, which can take different shapes from pin array, to stimulate the fingerpad, to a wearable vest or belt to provide a larger-scale stimulation. The process of transforming a mechanical force into neural signals is called mechanotransduction. This process, as the main responsibility of the haptic interface, plays a key role in determining how to generate and translate adequate mechanical force into a meaningful signal that the central nervous system (CNS) can relate to.

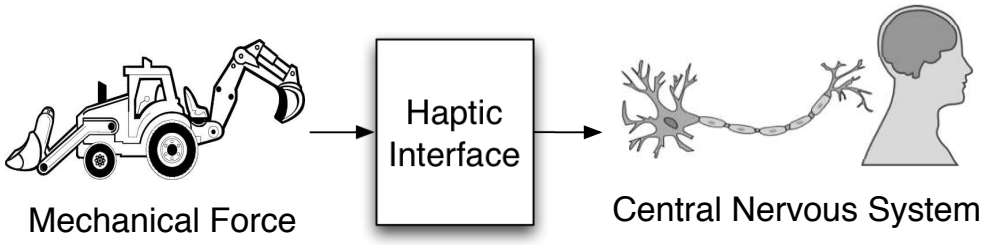

Fig. 2.1 Force, Interface and Central Nervous System

The way our body and mind respond to vibration cannot be described in a simple and predictable manner. From the mechanotransduction of oscillatory motion to the high-level interpretation by the central nervous system of the stimuli, every step is a different set of challenges and questions yet to be solved. This literature review focuses on the three

aspects of mechanotransduction. Reviews on vibrotactile devices, interfaces and perception will be presented in the first few sections. The final section will be dedicated to how the laws of physics, especially gravity, is perceived by the CNS.

2.1 Vibration Producing Actuators

Electromagnetic motors come in literally hundreds of different shapes and sizes, each designed for a different application. Although they all produce movements and operate based on the same underlying laws in electromagnetics, each of them has a different size, weight and geometry and moves differently with distinct characteristics of its own. Because of the vast variety of electric motors, the following review is far from exhaustive; however, it provides a general overview of vibration-producing motors relevant to the topics in this thesis.

2.1.1 Basic Vibration Motor

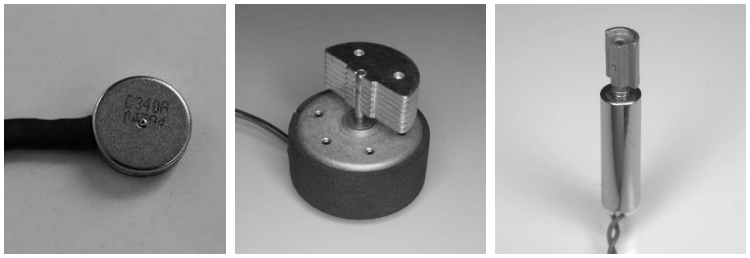

Fig. 2.2 Vibration Motors. From left-to-right: www.cibomahto.com, Precision Microdrives, Precision Microdrives

Vibration motors can be found in all cellphones and pagers capable of producing vibration notification. It consists of an off-centered mass attached to the shaft of a rotary DC motor and has the benefit of being very energy efficient and small. It is used in most mobile devices to provide vibration signaling. The disadvantage is the lack of control variables: the applied voltage determines directly the frequency and the amplitude of the vibration, and its bandwidth is very limited around the rotation frequency. To accelerate the off-centered mass, it may take up to hundreds of milli-seconds to ramp up to full vibration mode, representing a noticeable delay that requires compensation when precise vibration outcome is desired.

2.1.2 Voice-Coil Motors

Fig. 2.3 Voice Coil Actuators. Left-to-right: H2W Technologies, H2W Technologies, BEI Kimco Magnetics.

Voice-coil motors, also called VCM or magnetic actuators, are made using a similar principle as most linear motors and loudspeakers. They are widely used in the industry in many different areas, from robotic control and industry automation to consumer electronics. Despite the very different size and geometry, they all basically consist of voice coils, magnet and suspension mechanisms, and function by the Laplace force.

There are two kinds of voice-coil actuators: moving coil and moving magnet. The difference is that the former has the magnet fixed and the coil free-moving, whereas the latter has the opposite. The two configurations are sometimes used as alternatives for the same purpose, such as the phono cartridge of a turntable or industrial vibration shakers.

The moving-coil actuators have a light moving mass; hence, they have a low latency and can be controlled with great precision. They are often used in precision control such as in the head of a hard disk drive or as autofocus motors [1, 2]. One very specific application of voice-coil actuators is that of loudspeakers. The moving coil is connected to a membrane, which in turn vibrates to produce sound waves.

The moving-magnet actuators generally have the capacity to provide a greater output force due to the heavier moving mass. They also benefit from slightly simpler configurations because the moving part does not need electrical connection. This configuration is what is used in most tubular linear motors [3].

2.1.3 High-Power Shakers

Electromagnetic industrial vibration shakers are able produce high-amplitude, high-power vibrations. Generally used as test instrument, they are designed to produce controlled

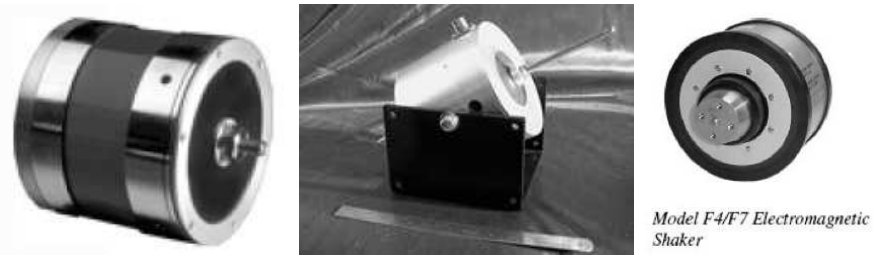

Fig. 2.4 Vibration Shakers. Left-to-right: Data Physics, MB Dynamics, Wilcoxon Research Inc.

vibrations of a large range of amplitude to test the impact of vibration on industrial equipment. Because of their high controllability, they have often been used in many past studies on vibrotactile perception. The downside is that they are usually very bulky and heavy, and thereby not suitable to incorporate into mobile devices.

2.2 Vibrotactile Haptic Devices

Vibrotactile actuators provide an energy-effective way to channel haptic information. There are many ways to stimulate the skin to create tactile sensation; a comprehensive survey can be found in the article by Khoudja et al.[4]. It can be direct stimulation, where the tactile actuator is in direct contact with the skin, or enclosure stimulation, where the contact area is significantly larger than the size of the actuator. Some studies use multiple vibration sources to simulate different places: either only the fingertip, the hand, around the waist or other places on the body.

2.2.1 Direct Stimulation

Direct stimulation is the most direct and simple way to create vibrotactile stimulus. In these devices, the actuator is usually in direct contact with the skin, through rigid coupling or through a surface not much larger than the contact area with the skin.

Tactors Tactors are small transducers that create tactile signals. When not specified, the term "tactor" is directly related to eccentric vibration motors. However, there are other types, such as voice-coil tactors, with a wider bandwidth.

Vibration motors, the most commonly used vibrating source, are made of a DC motor with an eccentric mass, as described earlier in this chapter. Its characteristic responses

were studied by Johns and Held [5]. Vibration motors are available in many different sizes and shapes. They are used in both direct and enclosure vibration paradigms. When used to create direct stimulation, one common choice is coin-shaped motors, around 10 cm in diameter and a few millimeters in thickness. They are sometimes called *shakers* or *vibrators* (mechanical), referring to the same motor. Despite the limited controllability and bandwidth, they are very popular because of their size, price and availability. They have been successfully used in many different contexts: mounted around the belt, the device can be used in directional navigation [6]; mounted inside a vest, they provide a non-intrusive way of communication that extends what vision and sound can provide [7]; mounted on the back rest of a chair, they form a low-resolution tactile array for letter reading [8]; mounted on a mobile device, they are used in the system "ComTouch", a multipoint vibrotactile display aiming to stimulate specific locations on the hand [9].

Voice-coil tactors have low inertia and can produce high-bandwidth vibration. They are often used to produce more refined tactile feedback that requires lower amplitude. A comparison between voice coil tactors and vibration motors can be found in the article by Niwa et al. [10]. Voice coil tactors have been used to: display vibratory feedback in teleoperation and virtual environments [11, 12]; give tactile feedback in digital musical instruments [13]; build a tactile array mounted on the forearm for perception experiments on signal identification [14]. These are just to name a few.

Mortimer, Zets and Cholewiak have developed a tactor specifically designed to directly stimulate the skin [15]. The vibrating "contactor" on the top of the coil-shaped actuator is to be placed against the skin. Their tactor is impedance-matched to the load of the skin, therefore capable of delivering stimulation in an optimal way. A few studies have used their tactor as the actuating element, such as the test bed designed to evaluate the effectiveness of tactile icons *Tactons* [16], or the development of the vibrating insole [17].

Flat Displays For portability reasons, many thin and flat tactile displays have been developed to be used in mobile technology. In the "Ambient Touch" system developed by Poupyrev et al., the actuating element is *TouchEngine*, a thin, miniature lower-power tactile actuator designed to convey localized tactile information directly on the skin for use in handheld devices [18, 19]. The contacting surface is a thin film made of piezoceramic material, which contracts of expands according to the input voltage. Another example is the "SmartTouch" system, which uses electrical stimulation applied directly on the fin-

gerpad through printed electrodes on the top of a circuit board [20]. On the bottom of the board, optical sensors are mounted in positions corresponding to each electrode. The sensor-actuator setup provides a compact integration of the sensing and displaying components. Another thin film tactile display is described by Yamamoto et al., in which the cutaneous stimulation is given when the user slides a thin film on a electrode plate [21]. The electrostatic tactile stimulation is capable of conveying surface texture, which is sensed primarily through movement.

Distributed Tactile Display To display high-resolution tactile detail, one single vibrating element is often not enough. Many high-resolution tactile displays consist of a matrix of pins, each actuated individually to apply a distributed force on the skin. The stimulation target is often the fingerpad, given its heightened sensitivity. To be able to display high-resolution tactile texture, the pins are often densely packed inside a square of a few centimeters. To drive each pin, several techniques have been used, such as shape memory alloy [22], DC motors [23], piezoelectric actuators [24], and electromagnetic actuators [25]. The pins are driven such to give a normal indentation to the fingerpad.

Hayward and his team have been developing distributed tactile displays to produce *lateral* stretch on the fingerpad. They suggest that within a limited range, normal indentation produces a similar sensation as lateral stretch. Several versions of the lateral stretch display were developed, in which each pin, made of piezoelectric bimorph, is actuated to produce lateral stretch toward the skin to display braille or tactile graphics [26, 27, 28].

2.2.2 Enclosure Vibration

Enclosure vibration is when the vibrating source is mounted inside an enclosure, and the skin contact is primarily the enclosure surface. This distinction is important as the enclosure is now an integral part of the device. The physical characteristics of the enclosure, such as its shape, size and weight, play a crucial role in the actuator choice and how the tactile signal is perceived.

Handheld Devices Handheld devices, such as mobile phones and PDAs, are the most common use of the enclosure paradigm. The enclosure is part of the whole tactile interface, and the choice of the source generator is generally made by taking the size and weight of the enclosure into consideration.

Mobile devices usually vibrate in pulses instead of continuously. Pulsing consumes less energy, is less annoying, and most importantly, adds another dimension to convey information. Kaaresoja and Linjama have experimented on how the signal duty cycle influences the annoyance [29]. Several applications for the pulsing signals have been developed, such as telling time [30], interactive racing games [31], and development of tactile icons "Tactons" [32].

Choi and his research group have done a series of studies on the very commonly used vibration motor in cellphones. Using a generic cellphone mockup and a common vibration motor, they have studied the power consumption along with the magnitude perception [33], and established methods of relating the relationship between the input, i.e. the applied voltage, to the output, i.e. the perceived magnitude [34, 35]. They also performed experiments on vibrotactile threshold and how the vibration is transmitted to the handheld devices with the device rigidly attached to an external shaker [36].

Linjama et al. demonstrated how to create a bouncing ball game using simple gestures, such as tilting and vibration feedback on a mobile phone [37]. Williamson et al. developed a multimodal interactive interface named *Shoogle* on a mobile phone [38]. As the user shakes or taps the device, he/she feels as if there are balls of liquid inside the enclosure.

Stylii Stylus provides a natural method of interaction in situations such as drawing and surface sensing. With accelerometers, Okamura et al. have recorded the vibration produced when tapping on a surface, stroking on a textured surface and puncturing a membrane using a sharp tool [39]. They found that high-frequency components recorded during these activities are often too high for many popular haptic devices to display properly. Vibrotactile signals are also used to display texture felt when dragging rigid probes on a surface. One popular stylus-based device used to render haptic texture is the Phantom from Sensable Technologies. It has a grounded base, capable of providing force feedback on a stylus. In the development of texture rendering algorithms, many use Phantom as a testbed [40, 41, 42, 43].

Ungrounded haptic stylus is often equipped uniquely with vibrotactile transducers. Although unable to provide non-vibratory force components, the ungrounded nature of these devices allows a larger workspace and a less restrictive interface. Poupyrev et al. have developed a way to provide haptic feedback for pen computing by moving the screen perpendicularly when the pen strokes over it [44]. Lee et al. present the design of a haptic

pen, equipped with a pressure sensor and solenoid, capable of producing haptic feedback in relation to the pressure sensed at the tip [45]. The same design has been used in devices designed for pen-paper interaction [46]. Yao and Hayward have developed a haptic-enabled surgical probe capable of enhancing surface texture when probing [47]. The same device is also used to demonstrate how it can be easily incorporated into an existing computer network [48].

2.3 Vibrotactile Perception

Research in vibrotactile perception has attempted to find out how vibration signals are perceived in relation to their physical parameters. Vibration arises naturally in our daily activities, such as clapping and writing; how it is sensed and represented in the central nervous system is essential to the overall understanding of human perception.

Another motivation to study hand-transmitted vibration is the well-known health hazard of prolonged exposure, such as hand-arm vibration syndrome [49]. Much effort has been put into studying various aspects of vibrotactile perception and how it is related to the severity of the vibration-induced syndrome.

There is a rich past literature focusing on how the physical characteristics of vibration, such as amplitude, frequency and vibration axis, affect the different aspects of perception, such as threshold, strength perception, frequency discrimination, or discomfort level. Examples of vibrotactile modality studied in the past are: whole body, hand-transmitted, foot-transmitted, on the fingerpad, and other parts of the body. This section of the literature review will focus on hand-transmitted vibration.

2.3.1 Mechanoreceptors

Tactile sensations arise when skin deformation occurs. Inside the skin can be found mechanoreceptors responsible for translating skin movement into neural code. Based on their morphology and their mode of operation, they are categorized into four groups: slowly-adapting I (SA I), rapidly-adapting (RA), and Pacinian corpuscle (PC) and slowly-adapting II (SA II). For vibrotactile sensations, RA afferents are responsible for low-frequency vibration, whereas PC afferents, with peak sensitivity at 200 Hz, respond mostly to high-frequency vibration. More detailed and extensive reviews can be found in Johnson's article on cutaneous mechanoreceptors [50] and Konietzny and Hensel's contribution on vibratory

sensitivity [51].

2.3.2 Detection Threshold

Vibrotactile perception threshold is the minimal signal intensity detectable by our sense of touch. It is highly dependent on certain characteristics of the signal and how the vibrating source is set up. From the frequency of 20 to 1000 Hz, the threshold level in terms of the displacement versus frequency yields a U-shaped curve with the lowest point (i.e. point of the maximum sensitivity) at around 250 Hz [52, 53, 54]. The curve is similar when testing with the hand holding a vibrating handle or applying the vibrating contactor directly on the skin [53, 55].

Another factor that affects this curve is the contact area between the skin and the actuator: it has been demonstrated that the larger the contact area, the lower the threshold [56]. The contact force seems to have little effect when the vibrating object is grasped by hand [57], and only for a certain frequency range [55, 58]. If the vibrating contactor has a static surrounding that is also in contact with the skin (i.e. the presence of contrast), the threshold becomes lower, especially in a low frequency range [55, 58]. Different vibrating axes have different sensation thresholds, but not in a systematic and a significant way [53, 59].

The threshold curve is also highly dependent on each individual and the test environment. It has been well established that older age is associated with a higher threshold curve [60, 61]; also, women have lower threshold values for higher frequency signals [62]. The temperature of the skin at the measurement location affects the detection threshold [62]. This extension of the influence depends on the frequency [55]. Hairy and glabrous skin have a different response curve, as the glabrous skin is more sensitive in frequencies above 20 Hz [63].

2.3.3 Strength Perception and Annoyance Level

Subject vibration strength perception is often measured by the method of magnitude estimation, in which the participants match the signal against a range of numbers chosen subjectively. Stevens first suggested that the relationship between the vibration amplitude and perceived magnitude follows a power function [64]. In 1969, Verrilo et al. performed several experiments on above-threshold strength vibrotactile perception [65]. They found

that: 1) the perceived strength is linearly correlated with the sensation level (in decibels) of the vibration; 2) in terms of the frequency, the perceived magnitude curve of signals slightly above the threshold values is similar to the threshold curve. As the signal level increases, the dip at around 250 Hz becomes less pronounced; 3) for the same signal level, women perceive it as stronger than men do, especially in higher frequencies. Older age is also associated with gradual lost of sensory ability. In short, the factors that affect the detection threshold also influence the strength perception. Similar studies have been performed by many other researchers for different conditions using different methods, resulting in slightly different but similar perception curves [66, 67, 68, 59, 57].

In acceleration and frequency plots from just above the threshold level, the equivalent-perception curves gradually change shape from the U-shaped curve into a more smoothly increasing curve. The discomfort level follows a similar trend as the equal-perception curve, except it is at a higher signal level [69, 53].

2.3.4 Signal Discrimination

Both hairy and glabrous skin was reported to have similar abilities to perform frequency discrimination, despite the different detection threshold [70, 71]. As the frequency increases, the absolute discriminative increment Δf also increases, but the ratio $\Delta f/f$ remains approximately constant, with a slight declining tendency.

The ability of the finger tip on differentiating tactile waveforms is also frequency-dependant [72]. At a low frequency (10-30 Hz), different waveforms are more discernible than at a higher frequency (100-300 Hz). However, the ability to perform intensity discrimination does not seem to be related to signal frequency and bandwidth. Weber's law, including the 'near-miss' of Weber's law, has been found to be applicable for the intensity discrimination task in touch [73].

2.3.5 Prior Exposure

Prior exposure to vibrotactile signals can affect the tactile sensation, causing higher detection thresholds and lower tactile sensitivity. The level of the sensory depression, also called vibrotactile adaptation, depends on the magnitude, frequency and duration of the vibration [74, 75]. It has been shown that the temporary threshold shift of vibratory sensation (TTSv) and vibrotactile adaptation can be explained by the lesser excitability of

the mechanoreceptive afferent units [76, 77]. This is precisely the reason why the detection threshold is an important measure to assess vibration-induced neuropathy [78].

2.4 Tactile Perception through Vibration

In the daily haptic interaction with the environment, vibration signals arise constantly. For example, when writing with pen and paper, they tell about the quality of the paper; when striking a ball with a racket, they tell about the impact and help to predict the trajectory of the ball; when shaking a jar of candies or liquid, they let us know if the container is full or empty. We can feel vibrations up to a few hundred hertz, and this wide range of sensing capability allows us to gain understanding about our environment.

2.4.1 Texture Perception

The texture is one of the first attributes that our sense of touch assesses when holding an object. Katz, a pioneer in the study of touch, first noted that there were two sets of essential cues for assessment of tactual texture: temporal and spatial [79]. He argued that the perception of texture is primarily determined by *spatial encoding* for coarse texture, and *temporal coding* for fine texture. This theory is called the *duplex theory of tactile texture perception*.

Katz's duplex theory was validated by experiments performed only one century later. First, evidence of spatial coding was found by Lederman in a series of studies, in which the perception of texture roughness is primarily determined by the spatial characteristics and is independent of the velocity of the moving finger [80]. Evidence of temporal coding was brought up by Cascio and Sathian, as they established the important role played by lateral movement in an adequate perception of the texture roughness [81]. Hollins et al. were able to provide a direct link between the vibrotaction and the perception of fine texture, by demonstrating that vibrotactile adaptation impairs discrimination of only fine, not coarse, texture [82]. In a separate article, Hollins et al. argued that vibrotaction is both necessary and sufficient for the perception of fine tactile textures [83]. Gamzu et al. also investigated the role of temporal cues in the perception of tactile spatial-frequency discrimination, showing that temporal cues are essential to this task, and that the strategy used by each may vary considerably [84].

In addition to the level of roughness, many other characteristics are attributed to the

surface texture, such as soft/hard, sticky/slippery, light/heavy, etc. Several past studies were carried out to uncover the perceptual dimensions of tactile textures, and demonstrated that it is highly complex and subject dependent [85, 86].

Besides using bare fingers, it is also possible to perceive texture using an instrument such as a rigid probe. However, the two modes of exploration are inherently different. When scanning using a probe, the predominant transmitted signal is vibration. When scanning with a bare finger, the deformation of the skin provides spatial information on the texture, which is not available when using a rigid rod. Klatzky and Lederman carried out experiments showing that, although not as good as bare hands, participants were able to perform the task of texture discrimination using a rigid probe [87]. In a follow-up study, Klatzky et al. examined how the probe and surface geometry and the exploration speed influence the perceived roughness [88]. They found that the "resolution" of the perceived roughness is limited by the tip size of the probe. Other aspects of tactual texture such as hardness and stickiness perceived using direct or indirect (i.e. through a probe) touch were looked into by Yoshioka et al.; they suggested that, given how different the texture information is perceived and processed neurologically, the two scanning modes rely on different neural mechanisms on the texture perception task [89].

2.4.2 Impact

When tapping on a surface with a stylus, we can tell a lot about the surface material based on the vibration generated by the impact. Okamura et al. analyzed the signals from tapping on different real materials and proposed the use of reality-based models to generate vibrotactile feedback [12]. Using this data, similar models were successfully implemented later by matching the sensed and outputted acceleration to improve contact realism [90]. Sreng et al. performed analysis of the vibration to the hand when hitting a target with a rod, and suggested that one can associate the vibration with the location of the impact [91].

On a larger scale, when hitting a ball with a bat or a racket, the haptic stimulus transmitted during the impact contains information about how and where the ball is hit. The optimum location of impact is called the "sweet spot". For a baseball bat, when the ball hits the "sweet spot", the vibration transmitted to the hand is reduced such that the batter is almost unaware of the impact [92].

2.5 Perception and Laws of Physics

This literature review has so far shown how the vibrotactile signal has been used to elicit haptic sensation, as well as how important the vibration is in tactual perception. Vibrotactile devices can not only directly contribute to vibrotactile perception studies, but also realistically recreate the real world in a virtual environment. By manipulating the virtual environment, we can create situations that cannot exist in the real world, and thereby provide means to probe further into human perception and cognition.

Our perception of the world emanates from information provided by our senses. The low-level perception serves as the basis for our central nervous system to perform high-level tasks such as extrapolating abstract concepts, drawing conclusions and making connections. Through interaction in everyday life, we are capable of acquiring an intuitive understanding of the basic laws of physics that govern the world around us. O'Regan and Noë's theory on sensorimotor contingencies argues that perception is a result of active exploration of the environment, and that continuous and engaging interaction is key to how "human experiences" come to life [93]. Environment invariants become recognizable once sensory and motor patterns follow each other consistently and lawfully [94].

2.5.1 Internal Model

Knowing and mastering the laws of motion is crucial to survival in general. When performing time-critical tasks such as striking a baseball with a bat, given the delay in the sensorimotor loop and the complexity of the computational task, it is very likely that the CNS resorts to more efficient strategies. The theory of internal model states that the CNS emulates the laws of physics for motor control and sensory processing. Using pre-existing internal models, it is then possible for CNS to make appropriate predictions and anticipations. Evidence of the existence of such models was suggested following experiments carried out by Wolpert et al. [95].

2.5.2 Gravity as a Physical Invariant

Among the laws of physics, gravity is an important constancy that affects every motion on earth. Merfeld et al. observed that, after being exposed to linear acceleration, subjects' eye movements contained a component that compensated for the acceleration even after the

acceleration had stopped [96]. Their results provided direct evidence of the role of internal models in estimating the effects of gravity.

Gravity is one of the first constancies learned in infancy. All parents of young children can testify the fascination of a 10-month-old when watching a toy falling on the ground (and dropping it repetitively). It was observed that infants as young as seven months old looked longer at recordings of gravity-defying events compared to gravity-following events [97].

One task that demands prior knowledge of gravity is intercepting falling objects: comprehensive reviews of past literature can be found in the articles by Zago and Lacquaniti [98] and Zago et al. [99]. The majority of past studies on object interception support the hypothesis that the laws governing movements on earth are internalized and as an event-independent perception invariance [100]. Examples of object interception experiments performed include under microgravity [101], inside a functional magnetic resonance imaging (fMRI) scanner [102], and blindfolded catching [103]. This is just to name a few.

As mentioned in the review paper by Zago et al. [99], the object interception task is almost exclusively dealt with in the visual-motor paradigm. To the author's knowledge, the only experiment performed without visual information input is the blindfolded catching experiment [103]. It involves playing sounds with the velocity encoded in pitch, an experience unlikely to occur naturally.

2.6 Summary

To bring haptics to ambient systems, one needs a suitable haptic actuator and a good understanding of human perception, two areas that this literature review focuses on.

One of the most economical and straightforward methods to create vibrotactile sensation is using electric motors. The most widely used vibration motors are rotary DC motors. They are small and inexpensive, but lack bandwidth capability and controllability. As an improved substitute, electromagnetic voice-coil motors seem to be a very good fit because of their controllability and versatility. Nevertheless, to the author's knowledge, among the off-the-shelf voice-coil motors with an acceptable level of vibration output, none is made in the size and dimension suitable for a hand-held vibrotactile display.

Many past studies have attempted to provide a solution for the lack of high-quality tactile feedback in handheld devices. Different technologies have been developed such that the actuator is in direct contact with the skin, for example a flat film mounted on the

side of the device or distributed display for the fingerpad. An alternative way of delivering simulation is to use the enclosure as a medium to deliver the vibration: most commercial mobile devices, as well as many research projects, use the simple vibration motor in this *enclosure* paradigm. A way to fill the gap among the range of choice could be a voice-coil actuator delivering enclosure vibration. Such a device is what will be proposed in Chapter 3.

Various aspects of vibrotactile perception have been studied in detail in the past: the detection threshold, the equal sensation contour, the annoyance level, the signal discrimination, etc. How vibration is perceived is affected by factors such as the vibration frequency and intensity, prior exposure, temperature, age and gender. Most of the past literature has been based on vibration produced by grounded devices, such as power drills or steering wheels. For mobile, ungrounded devices, the pertinence of the past studies is yet to be examined and validated. Chapter 4 and 5 will describe a series of experiments on how the device weight and signal frequency affect the perceived strength. The experiments attempt to contribute to a more comprehensive understanding of ungrounded vibrotactile devices.

Humans encounter vibrotactile signals from not only working with man-made machineries, but also interacting with the environment on a daily basis. This interaction, in addition to other haptic, auditory and visual experience, allows our CNS to gain understanding about laws of physics, hence the internal model for physics constancy. One of the most important physics constants governing every motion on earth is gravity. Many past studies had made important discoveries about how gravity is represented in our CNS, primarily based on the paradigm of object interception, a task requiring visual-motor integration. Using a vibrotactile actuator in an ambient haptic system, Chapter 6 will recount how experiments using a realistic haptic simulation of a rolling ball may provide evidence about the internal model of gravity in the *haptic* domain.

Chapter 3

A Voice-coil Vibrotactile Actuator for Haptics

Vibration signals can easily be generated using electrical motors. However, to produce controlled, high-bandwidth vibration while keeping the motor small and light-weight is far from a trivial task. Oftentimes, a tradeoff between cost, performance and size is inevitable. For instance, the vibration motor used in consumer portable devices is small and efficient, but has limited bandwidth capability. Another example is the commercial vibrations shaker used in most studies on vibrotactile perception as the source generator. These shakers, capable of producing high-amplitude and low-distortion signals, are mostly used in the test environment because of their large size and weight.

This chapter presents the analysis and modeling of a custom-designed vibrotactile actuator. Its theoretical model, the experimental frequency response, as well as the effect of each parameter on the output vibration are detailed in the following manuscript. The actuator serves as the vibration shaker in the experiments presented in later chapters. The manuscript enclosed below will be submitted to the *Journal of the Acoustical Society of America*.

Design and Analysis of A Recoil-Type Vibrotactile Transducer

by Hsin-Yun Yao and Vincent Hayward

Abstract

This article describes a new design of a high-bandwidth vibrotactile actuator and its modeling and analysis. The *Haptuator* can display wide bandwidth signals and has been used in several published studies. The transducer was modeled by converting its mechanical free-body diagram into equivalent electrical circuits. The experimentally obtained transfer function was combined with the function established theoretically to obtain the impedance expression for each parameter. Analysis is also performed to examine how changing each parameter's value affects the output performance.

3.1 Introduction

Modern portable communication devices are noted for their ever-increasing data processing and display capabilities. With mixed success, they strive to tap into several human sensory channels: vision, audition and touch. Comparatively, the use of the haptic channel—where movement and touch sensations are combined—in order to exchange information is achieved today only at a very basic level, as discussed in recent surveys [104, 105].

The only tactile feedback signal widely used in consumer applications is the vibrotactile signal communicated to the user by inducing persistent or transient oscillations to the enclosure or to the front plate of a hand-held device, delivering *enclosure vibration*. During operation, these surfaces are normally in contact with the fingers of the user, which makes these approaches very practical. Even when not in direct contact with the hand, for example, when the device is in a pocket or handbag, the large surface of the enclosure makes it possible to radiate sufficient vibration energy for an alert through layers of clothes or other material. Understandably, this type of signal is easy to create and can elicit relatively salient sensations in exchange of very little electrical power while occupying a tiny space and a small cost budget.

Another vibrotactile stimulation approach is to directly stimulate a small region of skin

tissue, as employed by *tactors*. They often operate like an acoustic transducer. While the tactor has more than eighty years of history since R. H. Gault noticed that the vibration of the membrane of a telephone earpiece caused strong cutaneous sensations, [106, 15] it has not been adopted by the consumer industry. This lack of adoption is likely to be due to the necessity to maintain direct contact between the radiating element and the skin through the use of a strap or of a garment. With the tactor, the regions of stimulation are also restricted to areas that are free of manipulative or sensing purposes, excluding, for instance, the fingertips and the thenar region, which are crucial during interaction with a device.

Enclosure vibration, on the other hand, is almost universally used in portable phones and other devices because it is practical. Oscillations are almost always obtained using vibration motors because they are very efficient in power and space and are easy to commission. Their efficiency arises from their mode of operation which is to spin an eccentric mass attached to the shaft of a DC motor. However, their expressive capabilities are—by principle—restricted, as further discussed in the next section. Despite its limitations, it is possible to use vibration motors in direct contact with the skin, making a "one note" tactor out of a vibration motor [5].

In this paper, we describe an alternative approach that relies on the enclosure vibration paradigm like the vibration motor, but is capable of producing precisely controlled vibrations over a wide frequency bandwidth like the voice-coil tactor. This transducer operates from a recoil principle by establishing a Laplace force between an elastically guided slug—a permanent magnet—and a tubular shell that contains two coils in an open magnetic circuit arrangement.

This transducer can be integrated in hand-held devices since, unlike voice-coil-driven tactors, it does not require a mechanical ground to operate and, unlike the vibration motor, has all the features of a transducer capable of large linear operating range. From a tactile display perspective, an analogy can be drawn with visual displays. Black-and-white binary displays are quite useful, say to display numbers, but color images are more visually appealing and capable of displaying realistic pictures. A wide-bandwidth transducer offers a wide range of vibration waveform choices, thus gives total freedom in interaction design.

In this article, after a brief background discussion, we present the transducer's working principle and its model by a free body diagram and its equivalent electrical circuit. We then describe a system identification procedure where each component of the circuit is obtained

either experimentally, theoretically, or both. The model is employed in the analysis of how changing the component's value affect the complete system performance.

3.2 Background

3.2.1 Basic Vibration Motor

For purposes of comparison, we first describe briefly the mode of operation of vibration motors. Refering to Fig. 3.1, a common design is when an eccentric mass is attached to shaft of a small DC motor. Sometimes, the design is integrated as in the model shown in the right most panel of Fig. 3.1.[107]

Fig. 3.1 Vibration Motors. From left-to-right: Precision Microdrives, Precision Microdrives, cibomahto.com

Consider the case when such motor is attached to a rigid mechanical ground. When the motor spins, the interaction force with the ground depends on the square of the angular velocity, which typically targets the range 100–200 rotations per second. [108] This method makes it possible to vibrate heavy loads provided that dissipative effects do not dominate the small power of the motor. Given a voltage step input of magnitude h, the spinning velocity follows a first order response, $\omega(t) \propto h[1 - \exp(-t/\tau)]$, since the vibrator obeys the general dynamic behavior of a DC motor where the time constant, τ, depends on the ratio of its inertia to its back-emf coefficient (the electrical time constant is negligible). The resulting centrifugal force is of the form $|f| \propto \omega^2$.

If the vibrator is mounted on a case much heavier than the spinning mass, then the vibration obeys $h^2[1-\exp(-t/\tau)]^2 \exp\{jh[1 - \exp(-t/\tau)]t\}$, where the vibration amplitude (the first factor) and the frequency (the exponent) are linked. If we plot the response of a typical vibration motor powered up to the full amplitude, we obtain a profile such as that seen in Fig. 3.2(left) where the ramp-up period is in the range of hundreds of milliseconds. This delay is noticeable and especially undesirable when a precise sensory outcome

is necessary. In fact, these motors are not suitable for scientific experiments that require stimulus with precise temporal properties.

To better visualize the restriction such a motor may impose on the interaction design, Fig. 3.2(right) shows the response of the same motor when the input voltage step is five times lower: the vibration frequency and amplitude are both significantly reduced. To overcome this limitation, some have considered adding additional dynamics to this kind of vibrators, [109] or using more sophisticated control schemes. [110] Nevertheless, the scope of these improvements is limited.

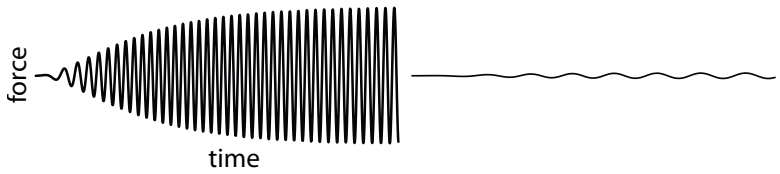

Fig. 3.2 Left: Chirp-like response of vibration motor to a step voltage input. Right: reducing the input amplitude by a factor of five renders a significantly slowed and weakened response.

3.2.2 Moving-Coil and Moving-Magnet Actuators

Moving-coil actuators (one model is represented in Fig. 3.3(left)) use the same principles as electromagnetic loudspeakers. They comprise a voice coil, a magnet creating an annular field, and a suspension mechanism. Below saturation, the output force is by and large linearly determined by the input current. They can be very accurate and do not have bandwidth limitations other than their structural dynamics and the ability of the driving amplifier to deliver current in an inductive load.

Compared to vibration motors, they are more expensive and generally larger, unless designed to operate at one single resonant frequency. In the latter case, their response magnitude is very sensitive to the presence of any dissipative term in the load, which is very detrimental to their role as a transducer. For haptic applications, moving-coil actuators are ideal. Often designed to move very small masses, they cannot produce large movements within the frequency range optimal for haptics, let alone be embedded in a portable device.

Moving-magnet actuators are designed to operated with a fixed coil and a moving magnet, which generally results in a larger output force for the same volume since a fixed coil

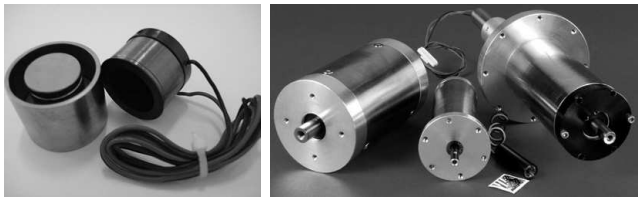

Fig. 3.3 Voice Coil Actuators. Sources, from left-to-right: Moving Coil (USAS Motion), Moving Magnet (H2W Technologies).

can be thermally connected to an external heat sink (models represented in Fig. 3.3(right)). The downside is a larger moving mass and often a more limited displacement range.

At a larger scale, permanent magnet linear actuators are widely used in vibration-generating test equipments or in air compressors. [111, 112] At a small scale, it can be produced with sub-milimeter sizes to use as precision actuator. [113, 114] Because of its simplicity and efficiency, it has a wide spread industrial and research application. Experimental and analytical modeling, optimization, improvements have been extensively discussed in the past. [3, 115, 116]

3.2.3 Other prime mover techniques

For vibrotactile haptic applications, other actuating principles have been explored: piezoelectric benders [117], stacks [118], and magneto-striction. None of them have the potential and the practicality close to those of electromagnetic actuators in either moving-coil or moving-magnet configuration.

3.3 Actuator Description

3.3.1 Physical Description

The proposed actuator, henceforth named an "haptuator", is a ungrounded moving-magnet voice-coil linear actuator. Referring to Fig. 3.4, a cylindrical magnet is suspended by two rubber membranes (in gray) via two non-ferromagnetic holders (hashed lines) inside a tubular enclosure (hashed lines) equipped with two sets of coils. The configuration is such that the generated magnetic field lines intersect the two coils at mostly right angle. When the current flows through the coils, it interacts with the magnetic field of the permanent magnet to create a Laplace force in the axial direction. The magnet moves axially and

relatively to the enclosure as a result of this force. The displacement is a function of the Laplace force, the dynamic intertial forces acting on both the enclosure and the magnet, and the viscoelastic forces resulting form the coupling between the two.

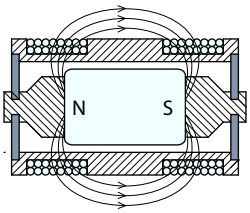

Fig. 3.4 Actuator arrangement. Shaded parts are made of non-ferromagnanetic material. A magnet is suspended by two rubber membranes in gray. The field lines intersect each coil to create an axial force. The coils are arranged such that the current flows in opposing directions.

Typical dimensions of the actuator can be rather small. The authors have made extensive use of a version that is 13 mm in diameter, 25 mm in length, see Fig. 3.5, and yet is able to produce several G's of acceleration given 5 W of input power. Similar designs have been used in several previous studies [47, 119, 48, 108]. Typically, the actuator was embedded in other enclosures or in the handles of larger devices. The coils are designed to have a 5 Ω impedance such the actuator could be powered with a common audio amplifier.

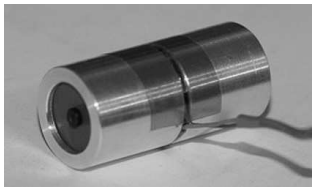

Fig. 3.5 External aspect of a 13×25 mm 'haptuator'.

3.3.2 Dynamic Model

Given the magnetic flux density $B(l)$ at a location l, and the current i at the location, the resulting Laplace force f can be described as:

$$f = i \oint dl \times B(l) = \gamma\, i, \tag{3.1}$$

where γ represents the actuator's drive factor, or the Bl factor. With the magnetic field of the permanent magnet, and the current in the coil, the Laplace force, like in a loudspeaker, emerges betwen the coil and the magnet.

The actuator is designed to operate without a mechanical ground. Its typical mechanical behavior can be represented by a six-parameter model, as shown in Fig. 3.6. An electromechanical force is applied to mass M_h, representing the equivalent inertia of the coil assembly, the device enclosure and the apparent hand mass. A force of the same magnitude and opposite direction is applied to a second mass, M_s, representing the inertia of the slug/magnet. These elements are connected by spring-damper systems, where K_s, B_s represents the suspension and K_h, B_h represents the external load. The positions of the masses are denoted x_s and x_h, respectively.

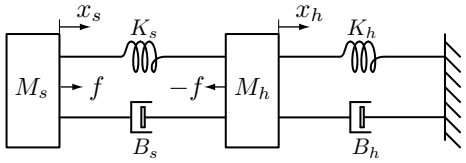

Fig. 3.6 Free-body diagram of the actuator. The two masses are free-floating. The 's' parameters can be set by design. The 'h' parameters represent the load to be driven.

Electrically, the system can be represented by the circuit shown in Fig. 3.7, with the voltage v, the current i, the voltage resulting from Lenz' law v_e, the actuator constant ϵ, the coil resistance R and the coil inductance L.

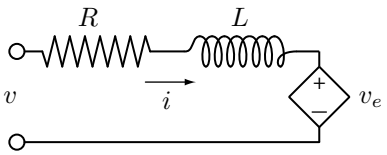

Fig. 3.7 Electrical circuit.

From these diagrams, the system's governing equations can be written as follows:

$$f = M_s \frac{\mathrm{d}^2 x_s}{\mathrm{d}t} + B_s \frac{\mathrm{d}(x_s - x_h)}{\mathrm{d}t} + K_s(x_s - x_h), \tag{3.2}$$

$$\begin{aligned} -f = M_h \frac{\mathrm{d}^2 x_h}{\mathrm{d}t} + B_h \frac{\mathrm{d}x_h}{\mathrm{d}t} + K_h x_h \\ - B_s \frac{\mathrm{d}(x_s - x_h)}{\mathrm{d}t} - K_s(x_s - x_h), \end{aligned} \tag{3.3}$$

$$f = \gamma i, \tag{3.4}$$

$$v_e = \epsilon \frac{\mathrm{d}(x_s - x_h)}{\mathrm{d}t}, \tag{3.5}$$

$$v = Ri + L\frac{\mathrm{d}i}{\mathrm{d}t} - v_e. \tag{3.6}$$

3.3.3 Equivalent Circuit

A practical approach to analyze mechatronic systems is to convert the mechanical part into an electrical equivalent circuit and connect to the rest of the electrical circuit. In systems that consist of components governed by mechanical, electrical, hydraulic, or acoustical laws, once each individual part is converted to equivalent electrical circuits, the whole system can thereby be represented by one single circuit. One can then use circuit theory to perform time or frequency analysis of the system. Such an approach has been extensively used to analyze acoustic transducers and enclosures. [120, 121, 122]

To find the equivalent circuit of a mechanical system, one can proceed using either impedance or mobility analogy based on the form of the governing laws in each domain. [123] After replacing the mechanical elements into its electrical equivalent using the conversion table 3.1, each element is connected in a way that satisfies the conservation laws. For example, using the mobility analogy, if two mechanical elements are subject to the same force, their electrical counterparts must be connected in series to share the same current; if they are forced to move at the same velocity, their counterparts must be connected in parallel in order share the same voltage drop. It must be nevertheless remembered that these analogies are mere tools for analysis and often lead to interpretations that do not possess a valid physical significance. [123]

From the mechanical free-body diagram, one obtains two equations describing the forces acting on M_s and M_h,

Table 3.1 Electrical equivalents to mechanical elements using the impedance or the mobility analogy.

Mechanical	Impedance	Mobility
Force f	Voltage v: $f \to v$	Current i: $f \to i$
Velocity $\dot{x}$	Current i: $\dot{x} \to i$	Voltage v: $\dot{x} \to v$
Mass M	Inductor L: $M \to L$	Capacitor C: $M \to C$
Spring K	Capacitor C: $K \to 1/C$	Inductor L: $K \to 1/L$
Damper B	Resistor R: $B \to R$	Resistor R: $B \to 1/R$

$$0 = M_s \frac{\mathrm{d}\dot{x}_s}{\mathrm{d}t} + B_s(\dot{x}_s - \dot{x}_h) + K_s \int (\dot{x}_s - \dot{x}_h) - f, \tag{3.7}$$

$$0 = M_h \frac{\mathrm{d}\dot{x}_h}{\mathrm{d}t} + B_s(\dot{x}_h - \dot{x}_s) + K_s \int (\dot{x}_h - \dot{x}_s) + f + B_h \dot{x}_h + K_h \int \dot{x}_h. \tag{3.8}$$

When employing the impedance analogy, an inductor L is a substitute for a mass M; the inverse of a capacitance $1/C$, for a stiffness K; a resistance R, for a damper B; a current i, for a velocity $\dot{x}$. The conversions are made such that equations that describe force balances become voltage loop equations,

$$0 = L_s \frac{\mathrm{d}i_s}{\mathrm{d}t} + R_s(i_s - i_h) + \frac{1}{C_s} \int (i_s - i_h) - v, \tag{3.9}$$

$$0 = L_h \frac{\mathrm{d}i_h}{\mathrm{d}t} + R_s(i_h - i_s) + \frac{1}{C_s} \int (i_h - i_s) + v + R_h i_h + \frac{1}{C_h} \int i_h, \tag{3.10}$$

$$0 = L_s \frac{\mathrm{d}i_s}{\mathrm{d}t} + L_h \frac{\mathrm{d}i_h}{\mathrm{d}t} + R_h i_h + \frac{1}{C_h} \int i_h \tag{3.11}$$

To obtain the electric circuit described by these equations, one considers them as the application of Kirchhoff's voltage law for two loops in a circuit. The current in each branch is then designated such that the three loops form a circuit shown in Fig. 3.8.

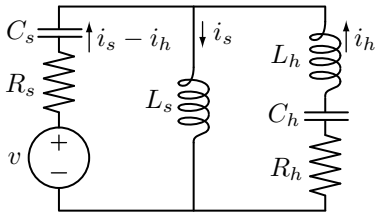

Fig. 3.8 Equivalent circuit using the impedance analogy.

Similarly, to use the mobility analogy, C is a substitute for M, $1/L$ for K, $1/R$ for B, voltage v for velocity $\dot{x}$, such that the equations that describes force equilibria become current summations at the nodes,

$$0 = C_s \frac{\mathrm{d}v_s}{\mathrm{d}t} + \frac{v_s - v_h}{R_s} + \frac{1}{L_s}\int (v_s - v_h) - i, \tag{3.12}$$

$$0 = C_h \frac{\mathrm{d}v_h}{\mathrm{d}t} + \frac{v_h - v_s}{R_s} + \frac{1}{L_s}\int (v_h - v_s) + i + \frac{v_h}{R_h} + \frac{1}{L_h}\int v_h, \tag{3.13}$$

$$0 = C_s \frac{\mathrm{d}v_s}{\mathrm{d}t} + C_h \frac{\mathrm{d}v_h}{\mathrm{d}t} + \frac{v_h}{R_h} + \frac{1}{L_h}\int v_h \tag{3.14}$$

The above equations can be viewed as the result of the application of Kirchhoff's current laws to three nodes of a circuit, where the current flowing through each element is equal to the voltage at its terminals divided by its impedance.

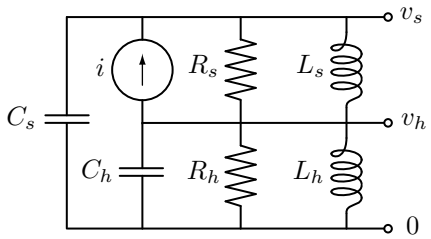

Fig. 3.9 Equivalent circuit using the mobility analogy.

To better visually compare the two analogies, related elements are grouped together in Fig. 3.8 and 3.9 to form the two circuits in Fig. 3.10. This summary figure shows the equivalent circuits of the mechanical system using the impedance and mobility analogies

(left and right, respectively). These transformations result in circuits that are dual to each other, and solving one is equivalent to solving the other. Note that for the impedance analogy, the values of the impedances are the inverse of the values for the mobility analogy ($Z \rightarrow 1/Z$) because of their duality properties. Despite the inverse relationship, all have the unit of Ohm (Ω).

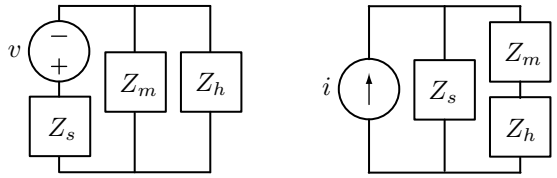

Fig. 3.10 Block representation of the mechanical components, left: impedance, right: mobility.

One important advantage of translating a mechanical system into an equivalent electrical circuit is that it can be combined with the electrical driver circuity, and the whole mechatronic system can be analyzed in a unified manner. Here we chose the mobility analogy, as in most loudspeaker analysis, mainly because effective force f is linearly proportional to the current input, therefore the coil impedance Z_c can be excluded from the calculation. However, choosing one analogy or the other is completely equivalent.

Using the mobility analogy, one may combine the circuit from the mechanical part with the electrical driver by mean of an ideal transformer of ratio $\gamma : 1$ (from (3.1)) as shown in Fig. 3.11. The induced current on the secondary side represents the force developed between the magnet and the coil. Since our setup employs a voltage amplifier, the input quantity is defined as the input voltage, and the output, the velocity or the acceleration of the external load. The relationship of $\dot{x}_h/v$ can be easily determined from the unified circuit. A similar approach is used in the analysis of loudspeakers driven by voltage amplifiers [122].

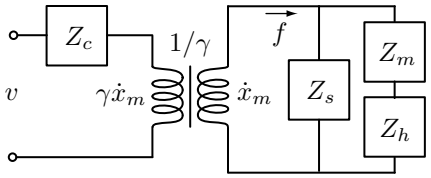

Fig. 3.11 Circuit representation of the electrical circuit combined with the equivalent circuit of the mechanical system.

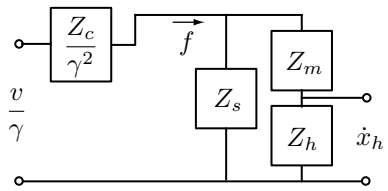

Fig. 3.12 Circuit representation of the combined system, replacing the ideal transformer by equivalent circuit.

One last transformation can be applied to the system representation to facilitate its analysis. Fig. 3.12 shows a circuit equivalent to that of Fig. 3.11 without the ideal transformer, by reflecting the primary side into the secondary side. Solving for the circuit variables now allows us to establish the relationship $\dot{x}_h/v$ and other variables of interest.

These transformations can be summarized by expressions in the Laplace domain ($s = jw$):

$$Z_c = sL + R, \tag{3.15}$$

$$Z_m = \frac{1}{s\,C_s} = \frac{1}{s\,M_s}, \tag{3.16}$$

$$Z_s = \left(\frac{1}{sL_s} + \frac{1}{R_s}\right)^{-1} = \left(\frac{K_s}{s} + B_s\right)^{-1}, \tag{3.17}$$

$$Z_h = \left(sC_h + \frac{1}{sL_h} + \frac{1}{R_h}\right)^{-1} = \left(sM_h + \frac{K_h}{s} + B_h\right)^{-1}. \tag{3.18}$$

3.4 System Identification

Some parameters such as the mass of the magnet M_s, the mass of the shell M_h or the input voltage can readily be known or measured. Some others, such as the mechanical impedance of the suspension Z_s and the actuator constant γ require experimental identification.

3.4.1 System Response and Modeling

In a first step, the input-output system response was measured when the load was just an inertia, that is, when $K_h = 0$ and $B_h = 0$. To achieve this condition, we secured the haptuator in a box and suspended it with thin threads. An accelerometer (ADXL320 from Analog Devices) was attached to the wall. When activated, the actuator could vibrate freely in the direction parallel to the floor, see Fig. 3.13.

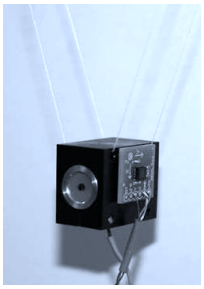

Fig. 3.13 Measurement setup with purely inertial load.

The acceleration response over the input voltage for three different input levels can be seen in Fig. 3.14. The responses for 1, 2 and 3 V (rms) do not fall exactly in top of each other, but differ only by less than 1 dB. This slight discrepancy is easily explained by saturation effects which are mostly noticeable around the natural resonance at around 60 Hz. Like for loudspeakers, the saturation effects are due to the large excursion of the moving part that 1) causes the suspension to cease acting linearly, and 2) makes the actuator to operate in a zone where the magnetic flux crossing the coils is no longer constant. For this input, the acceleration is overall 2.5-3 G throughout the frequency range. For a 1 V input (1 G output for this load), the actuator operates perfectly linearly. As a reference, most cellphones can deliver vibrations of up to 1.5 G peak-to-peak acceleration, a level often considered very strong perceptually and particularly hard to miss.

As expected, the shape of the response resembles that of a 2^{nd} order system with a 60 Hz natural resonance, the approximate location of the poles in the transfer function. It also decays following one slope up to around 150 Hz, and according to another from 150 Hz to 500 Hz, indicating the presence of a zero at around 150 Hz. A 2^{nd} order model with two poles and two zeros gave an excellent fit ($r^2 = 0.98$). It is written

$$\begin{aligned} \hat{H}(s) = \frac{\ddot{x}_h}{v} &= \frac{0.685s(s-1150)}{s^2+565.9s+1.283\text{e}5}, \\ &= \frac{as(s-b)}{s^2+2\zeta\, w_o\, s+w_o^2}. \end{aligned} \tag{3.19}$$

where the damping coefficient is $\zeta = 0.79$ and the resonance frequency $F_0 = \omega_0/2\pi = 57$ Hz. As seen in Fig 3.15, the model gradually differs from the measured response for frequencies above 400 Hz, indicating the possibility of one or several zeros at higher frequencies. The

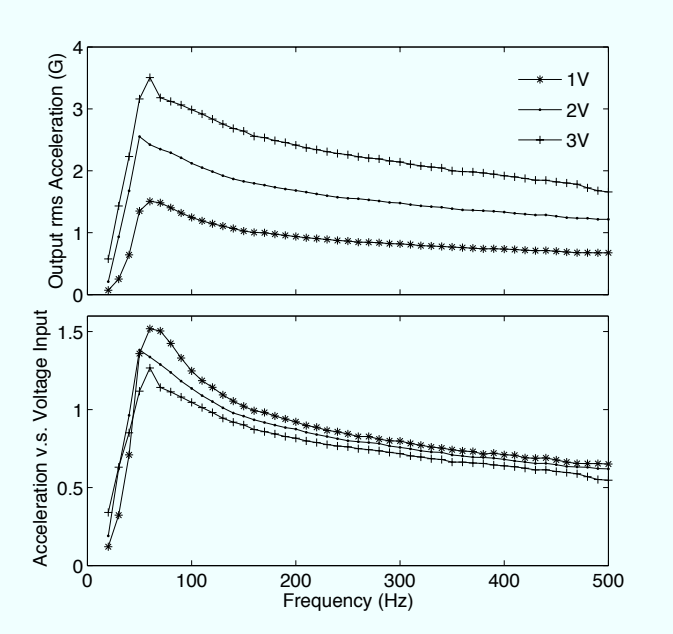

Fig. 3.14 Frequency response (rms) of the actuator acceleration to inputs of 1V, 2V and 3V (top) and the ratio for each level (bottom, in dB).

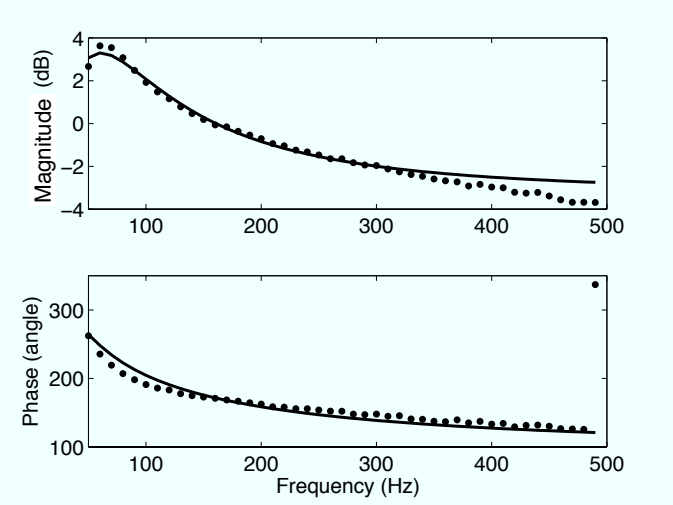

Fig. 3.15 The magnitude and phase plot of a fitted 2$^{\text{nd}}$order model.

additional zeros likely due to the accelerometer transfer function (rated bandwidth 500 Hz), but not to the actuator.

3.4.2 Parameters found independently

Due to the small number of turns, the inductance of the coil L (found to be $2.05{\cdot}10^{-8}$H) could be neglected in the frequency range considered, hence Z_c could be measured directly to be $Z_c = 5.0\ \Omega$. Other parameters directly measurable are the mass of the magnet, $M_m = 7$ g, and the mass of the case and of the test box, $M_h = 15$ g.

The actuator drive factor, γ, (or 'Bl' factor) was obtained using 2 methods: force measurement and finite element simulation.

The first method involved measuring directly the force produced by a DC current. The rubber suspension was removed, and a peg was used to keep the magnet centered. The actuator was placed vertically above a scale such that when a DC current was sent to the coil, the magnet produced a force acting against the scale. Having the force and the current, using equation (3.1), γ can be obtained.

The second method employed a commercial finite element analysis tool (COMSOL 3.5, COMSOL AB, Stockholm, Sweden). The geometry of the actuator was supplied to the simulation, as well as the B field of the magnet, measured to be 0.50± 0.01 T at the poles, and the total coil length. The software simulation tool used the above parameters to calculated γ. A plot of the magnetic field lines and the resulting Lorentz force from the simulation can be seen in Fig. 3.16.

With the first method, twelve measurements were made with $i = 70$ to 143 mA, and γ was found to be 0.98±0.06. The second method gave γ=0.96±0.01. These values are within each other's uncertainty range. In the following sections, the average value of γ=0.97 will be used.

Fig. 3.16 The magnetic field lines emanating from the magnet. The arrows show the forces acting on the coil.

3.4.3 Suspension Impedance

From Fig. 3.12, one can derive the transfer function from voltage input to output in terms of the system parameters. The output of the transfer function is defined as the acceleration of external load $\ddot{x}_h$ because it is an easily measurable quantity compared to the velocity $\dot{x}_h$.

$$\begin{aligned} \frac{\dot{x}_h}{v} &= \frac{\gamma Z_s Z_h}{\gamma^2 Z_s Z_m + Z_c(Z_m + Z_h + Z_s)} \\ H(s) = \frac{\ddot{x}_h}{v} &= \frac{s\,\gamma Z_s Z_h}{\gamma^2 Z_s Z_m + Z_c(Z_m + Z_h + Z_s)}. \end{aligned} \tag{3.20}$$

The quantities Z_s, Z_c, Z_m, and Z_h can be substituted in (3.20) for their expressions, (3.15)–(3.18), to give

$$\begin{aligned} H(s) &= \frac{s\,\gamma Z_s Z_h}{\gamma^2 Z_s Z_m + Z_c(Z_m + Z_h + Z_s)} \\ &= \frac{s\,\gamma(K_s/s + B_s)^{-1}(sM_h)^{-1}}{\gamma^2(K_s/s + B_s)^{-1}(sM_m)^{-1} + R((sM_m)^{-1} + (sM_h)^{-1} \\ &\qquad + (K_s/s + B_s)^{-1})} \\ &= \frac{s^2\gamma M_m}{s^2 R M_m M_h + s(\gamma^2 M_h + R M_h B_s + R M_m B_s) \\ &\qquad + R M_h K_s + R M_m K_s} \end{aligned} \tag{3.21}$$

The transfer function (3.21) is of 2^{nd} order with two zeros and two poles with two unknown parameters, K_s and B_s, which together describe a 1^{st}-order suspension model as in (3.17). Keeping Z_s, substituting in (3.20) the values M_m=0.007, M_h=0.015, γ=0.97, and R=5.0, the transfer function becomes

$$\begin{aligned} H(s) &= \frac{s\,\gamma Z_s M_m}{Z_s\gamma^2 M_h + R M_h + R M_m + s R Z_s M_m M_h} \\ &= \frac{64.7 s\, Z_s}{134 Z_s + 1.05e3 + 5.0 s Z_s}. \end{aligned} \tag{3.22}$$

An expression for $\hat{Z}_s$ can be found by relating (3.22) with the transfer function (3.19)

obtained experimentally,

$$\hat{Z}_s(s) = \frac{11.7\,(s - 1150)}{s^2 + 659s + 1.37e05}. \tag{3.23}$$

Instead of a 1st-order expression, $Z(s) = (K_s/s + B_s)^{-1}$ from (3.17), we find a more complicated 2nd-order expression. This can easily be explained by considering that the disk suspension operates as a vibrating membrane. Its actual dynamics are likely to involve high-frequency vibrations modes picked up by the experimental identification procedure in the frequency range of interest.

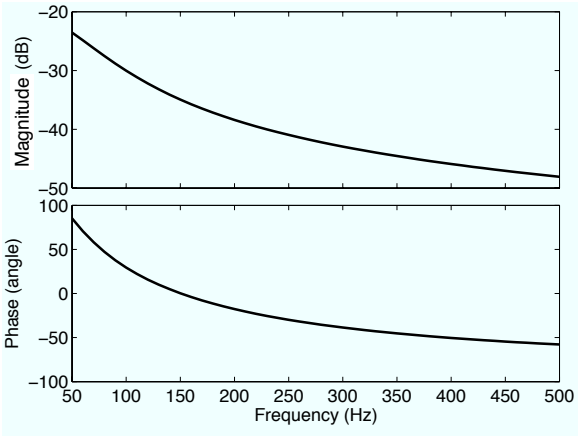

Fig. 3.17 Plot of the impedance of the suspension, Z_s as in equation 3.23.

The denominator of (3.22) suggests that the first term, $134\,Z_s$, is the dominant term for position of the poles. When comparing the response of Z_s in (3.23) (see plot in Fig. 3.17) to the model (3.19), it is noticed that they share the same zeros at 0 and 1 150 rad/s, and that they have poles that are very close to each other (358 vs. 370 rad/s). The resemblance between the transfer function and the suspension impedance suggests that the transfer function is largely determined by the characteristics of the suspension and shaped by the other parameters.

3.5 Actuator Analysis

The next step is to investigate, individually, the impact of each parameter on the overall outcome of the system. The effect of varying each element's value in (3.20) is presented in

this section, except the magnet mass Z_m. The magnet plays a key role in the dimensioning of the actuator, and changing it would mean changing the whole geometry of the actuator. It is therefore not suitable to be analyzed individually.

3.5.1 Impedance of the suspension: Z_s

As noted in the previous section, Z_s dominates the placement of the system zeros and poles. Physically, the suspension of the actuator is a thin rubber disk designed to be much more compliant in the axial direction than in the radial direction. At high frequencies, it behaves like a membrane with vibration modes that gave to Z_s a 2^{nd}-order transfer function characteristic (3.23).

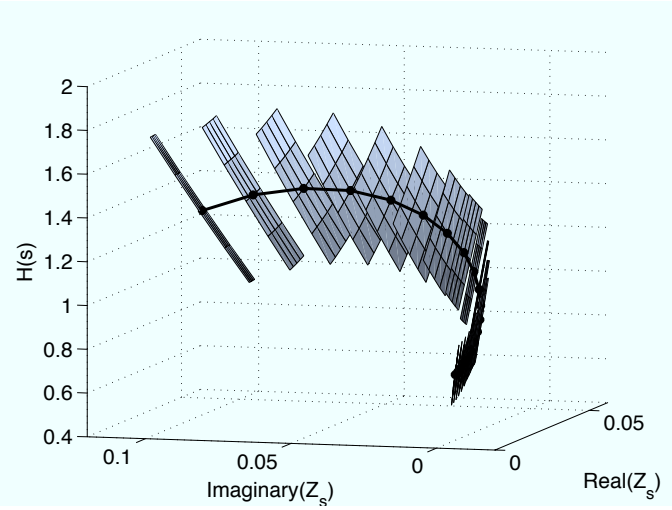

Fig. 3.18 Each surface represents the magnitude of H(s) for different values of Z_s in the complex plan from 50 Hz (leftmost) to 500 Hz. The surfaces show the change of $H(s)$ when Z_s varies by $\pm 20\%$ around a given value.

The modification of the material and of the thickness of the suspension changes the acceleration response of the actuator according to (3.22). Figure 3.18 shows the variation of $H(s)$ when Z_s varies by 20% around a nominal value. Each point on the horizontal surfaces corresponds to a value of Z_s and the height represents the magnitude of $H(s)$. The relative change of $H(s)$ decreases with increasing frequency, 23% at 50 Hz and 18% at 500 Hz. This shows the response is more sensitive to variations of Z_s in the lower frequencies.

3.5.2 Load Inertia Z_h

The goal of this actuator is to provide a source of vibration to an external load. Fig. 3.19 shows how different inertia of the external load affect the acceleration output, based on (3.20). As might be expected, the acceleration output decreases with a larger load. The phase plot, however, is unaffected when Z_h varies from 15 to 100 g. Fig. 3.19 plots the results for the holder mass of 15 to 100g in 5 g increments. The higher the mass, the denser the lines, which means that the magnitude doesn't decrease linearly with the increasing mass. The higher the mass, the less the incremental effect on the output decrease.

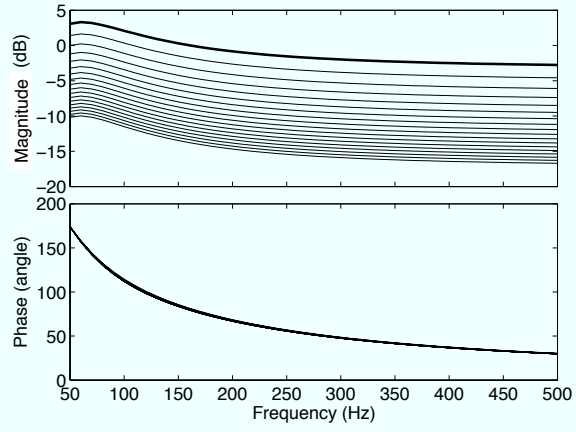

Fig. 3.19 Acceleration output when the load varies from 15 g (highest output) to 100 g with 5 g intervals. The thick line in the magnitude plot with the nominal value of 15 g.

3.5.3 Actuator drive factor γ

The factor γ is primarily determined by the B field and the coil total length. Figure 3.20 shows how a higher value of γ increases the response. Similar to Z_h and Z_c, the output magnitude is almost directly proportional to the increase of γ, while the phase remains unchanged.

The software analysis tool was used to investigate different strategies to increase γ without changing significantly the geometry, the size or the electrical characteristics of the haptuator.

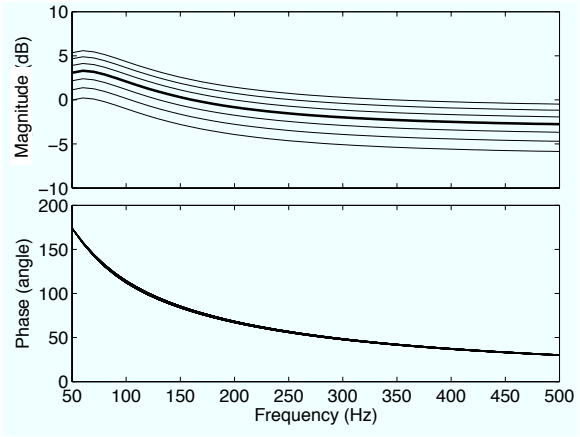

Fig. 3.20 Acceleration output for values of γ 30% higher (highest output) to 30% lower. Each line represents a 10% increment. The thick line in the magnitude plot with the nominal value, γ=0.97.

Coil Placement The coil of the actuator should be placed where the magnetic field is the strongest, which is when the mid-point of the coil is aligned with the edge of the magnet with a small offset, see Fig. 3.21. Although the field lines are the densest around the magnet edge, because the field is not completely symmetrical, moving the coil sightly toward the denser area increases the output force. Simulation showed that the optimal placement is when the mid-point of the coil is offset by about 0.4 mm with respect to the edge of the magnet.

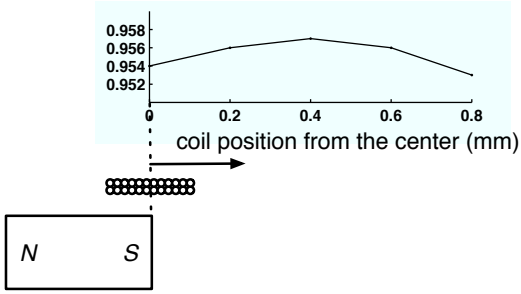

Fig. 3.21 Values of γ for different coil positions away from the center position.

Coil Configuration Another possible optimization is to attempt to pack as many turns as possible where the magnetic field is strongest. This can be achieved by shortening the coil

length and increasing the number of layers, while keeping the same total number of turns. A tradeoff exists since the field decays radially. Simulations demonstrated that γ improves with the number of layers until the coil thickness becomes large enough to prevent any further improvement. A thicker coil increases the actuator width, but decreases it length.

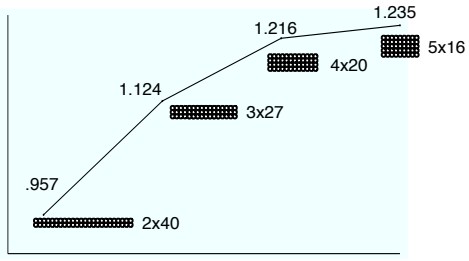

Fig. 3.22 γ given by different coil configurations.

3.6 Conclusion

The goal of this paper was to describe, model, and analyze a new type of recoil actuator operating under the same enclosure vibration paradigm as the common vibration motor, yet capable of producing wide-bandwidth vibrotactile signals. The model of the system was first determined by its mechanical free-body diagram, which in turn was translated into an equivalent electrical circuit such that it could be combined with the electrical driver to form a unified circuit. The transfer function of the complete system was measured experimentally and fitted into a 2^{nd}-order model. The experimental model was then combined with the expression obtained theoretically. While most parameters contributing to the transfer function could be measured independently, the suspension and the actuator drive factor γ were identified experimentally. It was verified that γ could be accurately predicted by simulation with finite element analysis tool. By substituting the experimental data into the theoretical equation, it was then possible to find the remaining unknown suspension model.

Having the model allowed us to perform analysis, for each parameter individually, on how changing the impedance's value may affect the overall response. Results showed that suspension characteristics impacted the response the most in the low frequencies. In that, the haptuator is similar to a loudspeaker. The other components had a direct and simple

effect on the performance. A higher value of γ increased the output proportionally, and a bigger inertia load diminished the output acceleration, as expected. As the finite element analysis simulation correctly predicted the factor γ obtained experimentally, it was also used to suggest optimization possibilities by changing coil/magnet geometry.

The next step is to probe further in how the performance would vary for the same actuator but of different sizes and dimensions. With the model of the system and assisted by the simulation tool, it would be possible to establish how scaling the actuator linearly or into other shapes, for instance like a coin or a thin rod, may affect its performance.

Acknowledgments

This study is funded by NSERC IPS award granted to the first author during her doctoral study. The authors would like to thank Jean-Samuel Chenard for participating in the actuator design and the mechanical prototype fabrication.

Chapter 4

Vibrotactile Perception in Mobile Devices: a Preliminary Study

Mobile devices, such as cellphones, pagers and PDAs, are undoubtedly the most common application of vibrotactile display. Despite the rich past literature on vibrotactile perception, few studies accounted for the aspects specific to ungrounded devices such as cellphones. Using the portable and high bandwidth actuator described in the previous chapter, it is now possible to fabricate an apparatus that: a) provides vibration of high enough bandwidth to study vibrotactile perception, and b) is small enough to be included in an enclosure of size and weight similar to common portable devices.

Two articles were published on the vibrotactile perception of mobile devices, both in collaboration with Immersion Corp. Included here is the first manuscript, a short report of a pilot study on how the weight of the device influences the intensity perception. It was published in the *Proceedings of Second Joint EuroHaptics Conference, and Symposium on Haptic Interfaces for Virtual Environment and Teleoperator Systems, 2007*. The second article will appear in the next chapter.

The Effect of Weight on the Perception of Vibrotactile Intensity with Handheld Devices

by Hsin-Yun Yao, Vincent Hayward, Manuel Cruz and Danny Grant

Abstract

The objective of this study was to determine whether the weight of a vibrating handheld object influenced the perceived intensity of its vibrations. Experiments were conducted to determine the subjective equivalence of vibrotactile intensity for objects that had the same size but had different weights. The results suggest that for the same surface acceleration and hence the same movement, the heavier the device is, the stronger the perceived intensity is.

4.1 Introduction

Vibrotactile signals are nowadays important for the design of a variety of handheld devices. To design them, it is important to know whether the perceived vibrotactile intensity depends on other object attributes, chiefly among them is weight. Despite a long history of vibrotactile studies we could find little data that was related to this question [73, 124, 61, 125, 126].

Most portable phones provide a vibrotactile function to signal a call. Design engineers must carefully select the actuator to fit a tight power budget. We observed however that the way a device felt in our hand seemed to depend on its weight, and this despite compensating

for the physics of vibration. This led us to hypothesize the existence of a weight-vibration perceptual interaction.

We carried out an experiment to determine the subjective equivalence of the vibration intensity for objects having different weights. We found that for the same acceleration, doubling the weight of an object resulted a perceptual sensitivity enhancement of about 2.4 dB.

4.2 Method

We manufactured boxes with weights and sizes similar to that of common portable phones. Each was equipped with a high-bandwidth actuator and an accelerometer attached to its surface. The method of adjustment was used whereby participants adjusted the vibrating intensity of a given box to match that of a reference box.

Apparatus. Four boxes (80 × 40 × 17 mm), along with their controlling circuitry, were made. The boxes weighted 50, 110, 200 g. A fourth 110 g box served as the reference. Each contained a custom-made, recoil-type Lorentz actuator made of a magnet suspended inside a pair of coils in an open magnetic circuit arrangement. It could accelerate a 110 g box up to 30 m/s^2 from 20 to 500 Hz with minimal distortion. The intensity was adjustable by turning a rotary control similar to that of audio equipment. Each had a calibrated accelerometer (MMA7260Q, Freescale).

Stimulus. We used sinusoidal vibrations of 150 Hz with amplitudes from 3 to 14 m/s^2. The signals were pulsed in a 0.5-second-on, 0.5-second-off duty cycle to minimize adaptation. The frequency, magnitude and the pulse-train signal approximated that of an actual portable phone.

Protocol. Eight healthy university students (4 males, 4 females) were recruited. During each session, the participants were seated in front of the four boxes which rested each on a block of soft gel. They were told that there was one reference box and 3 adjustable boxes. For each trial, the reference box and one of the tunable boxes would vibrate. They had to lift, feel the boxes, and then adjust the intensity of the tunable box until its vibration felt the same as the reference box. They wore sound-blocking earphones and used their

dominant hand only. When a participant was satisfied, she put both boxes back on their block of gel. The acceleration of each box was recorded and logged by computer before the next trial. Each participant was presented 20 pairs of stimuli in total, and they were asked to take a one-minute break after the 12th pair. All completed the experiment within 30 minutes.

4.3 Results

The results (acceleration r.m.s. converted to dB re 10^{-6} m/s^2), see Fig. 1, showed that the weight of the device influenced the perception of vibration magnitude. The data for each condition was fitted with straight lines. The control condition was when participants had to match intensity of boxes of the same weight. On average, they behaved almost like the ideal performer (thick line) for this condition. We calculated the normalized acceleration by taking the ratio of the matched acceleration over the reference acceleration. The ANOVA test performed for each of the three pairs of data (50 g vs 110 g, 110 g vs 200 g, 50 g vs 200 g) showed significant difference for all the pairs ($p < 0.001$). On the boxplot, the notch indicates a robust estimate of the uncertainty about the medians for box-to-box comparison. Since the notches do not overlap, the plot indicates the medians of each pair differ at the 5 % significance level. The results show that a heavier box requires less acceleration to produce the same perceptual effect than a lighter one.

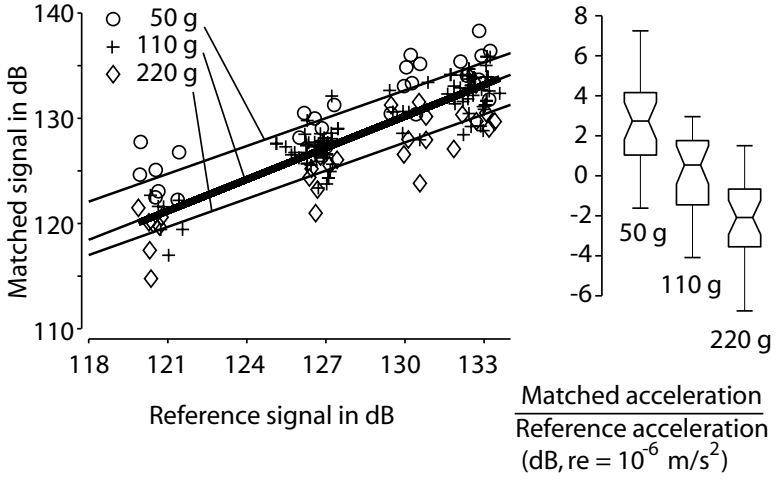

Fig. 4.1 Matched values versus reference values.

4.4 Discussion

Our results support the hypothesis that the weight of an object affects the perception of vibration magnitude. The heavier the box, the smaller is the required acceleration to produce the same perceptual intensity. One possible explanation is that when we hold a heavy box in our hands, we need to use a stronger grip, therefore the contact area between the skin and the device is larger than with a lighter box [56], which, in turn, stimulates a larger number of mechanoreceptors. A second explanation is that a heavier object can cause more tissues to vibrate for the same acceleration. A third explanation would appeal to psychophysical mechanisms [127]. Whatever the biomechanical, neurophysiological, or psychological factors may be, our nervous system translates this vibration pattern into the perception of stronger intensity.

The weights were specifically selected to have almost the 1:2:4 ratios. As seen in Fig. 1, the relative perceptual differences between the successive weights are almost the same: 2.4 dB between 50 g and 110 g, and 2.3 dB between 110 g and 200 g. This difference was relatively constant for all signal amplitudes within our range of testing. It means that, on average, for the range of weight between 50 and 200 g, to obtain the subjective equivalence for a device twice as heavy, one need to reduce by about 2.4 dB to the response of the original box.

4.5 Conclusion

We have found that the design of the vibrotactile signal given by a handheld device should take its weight into consideration. This result is potentially useful for the portable device industry as it provides a basic guideline for vibrotactile tactile transducers.

It is tempting to relate our findings to the well-known size-weight illusion [128]. Our present protocol makes an implicit causal connection between weight and the perception of vibrations as it is motivated by our application. It would be interesting to investigate whether a reverse interaction occurs.

Chapter 5

Vibrotactile Perception in Mobile Devices: the Follow-up Study

The previous chapter described the preliminary study on how weight affects the perceived vibration strength of mobile devices. This chapter presents a manuscript describing the results of two experiments: the first one as the follow-up, more extensive experiments confirming the results from the previous study, and the second experiment is on how the underlying frequency affects the perceived vibration intensity. The article was accepted in *IEEE Transaction on Haptics* in July 2009.

Perceived Vibration Strength in Mobile Devices: the Effect of Weight and Frequency

by Hsin-Yun Yao, Manuel Cruz and Danny Grant

Abstract

This paper addresses the question of strength perception for vibration signals used in mobile devices. Employing devices similar to standard cellphones and using pulsed vibration signals to combat adaptation effects, experiments were performed to study the effect of weight and underlying vibration frequency on perceived strength. Results shows that for the same measured acceleration on the device, a heavier box is perceived to vibrate with greater strength. Furthermore, signals with higher underlying frequency are perceived to be weaker for the same measured acceleration. While our results are consistent with previous studies, they are obtained for the specific condition of ungrounded, vibrating objects held in the hand. Our results suggest the need for a systematic correction law for use by designers to specify the vibratory characteristics of a device as a function of its weight and of the desired operating frequency.

5.1 Introduction

Providing notification through vibrations has been an important functionality of pagers and cellphones since their appearance in the consumer market. This haptic capability is an essential communication channel for mobile devices as it can be used to convey information privately to the user.

As the cellphone market continues to expand, it is increasingly vital for each component to be optimized. Haptic capability is not an exception: more efficient haptic signaling allows for greater use of the haptic channel for communication. The present paper tackles the

question of how the perceived vibrotactile strength can be influenced by different factors, and aims at providing insights into the creation of more perceptually efficient vibrotactile signals across cellphone models.

5.2 Related Work

Human perception of vibrotactile signals has been the subject of many studies since the miniaturisation of electromagnetic devices more than a century ago [106]. Many aspects of vibrotactile perception have been studied in great detail: detection threshold [53, 61, 54, 68], perception of strength and equal sensation curve [66, 129], frequency discrimination [70, 71], the influence of grip force [130, 57], level of annoyance [53], and others. Most previous studies, if not all, used devices that were rigidly fixed and subjected to continuous vibration signals. Magnitude estimation was performed with reference signal between 5-10 Hz, vibrating around or under 1 m/s^2 r.m.s (2.8 m/s^2 peak-to-peak).

Despite the rich literature in this area, few studies address the question of vibration strength perception in hand-held devices, even though there were over 1 billion mobile phones sold in 2007 alone. Mobile phones, and other similar devices, have perceptual characteristics that are noticeably different from the vibrating devices studied in the past. First, they are not mechanically grounded, and the motor task while manipulating the object is different than, say, when handling an electric drill. When a device can be moved freely, our hypothesis is that size and weight affect the perception of its vibration strength. In addition, past studies on perceived strength were done considering vibration as unwanted noise; whereas in mobile devices, the acceleration magnitude is relatively high, normally from 7 -20 m/s^2 peak-to-peak (0.7 to 2 times that of gravity). Here, the signals are meant to be perceptually significant, hence the greater range and value of accelerations.

Another distinctive aspect of these earlier studies was the focus on a very wide range of frequency using a reference frequency of around 60 Hz. This does not match the range of interest for current cell phones, which can extend up to 200 Hz. Furthermore, mobile devices have the ability to create complex pulsing vibration patterns, not just continuous vibrations. Pulsing techniques allow for a richer display of haptic effects, consume less power on average, and, most importantly, add another dimension to convey information.

Several studies regarding perception of vibrotactile signals for mobile devices can be found in [33, 36]. One of these studies was performed using a handheld device rigidly

attached to an external shaker, thus the device was not held in free-space and the stimulus was transient, not pulsing. The other was only applicable to the case where the vibration motor itself is placed on the thenar eminence. Kaaresoja and Linjama investigated how the vibration signal duty cycle can influence user annoyance [29]. Interesting applications for pulsing signals have been developed, such as telling time [30], interactive racing games [31], or development of tactile icons "Tactons" [32].

Weight is one of the important characteristics designers consider for mobile devices. Starting with Weber [131], the perception of weight has been a topic of research for 175 years. One of the most interesting and relevant phenomenon is the size-weight illusion. Charpentier first reported it over a century ago [128], and it has been studied many times after [132, 133]. However, still today there is no satisfactory explanation for it [134]. These studies showed that the magnitude perception of haptic signals is not related in a simple fashion to physical quantities. In particular, skin contact has an impact on the perception of weight. It is possible, for instance, to create or alter this perception by direct modifications of the contact conditions. Recently, there have been successful attempts to recreate the sensation of heaviness with haptic devices: by controlling the skin stretch [135], skin compression [136], or with asymmetric vibration [137].

5.3 Object and Motivation

In this paper, the influence of two factors on the perception of strength were examined: the weight of the device and the frequency of the driving vibration. Since we found clear correlations between these factors and the perception of vibration strength, our findings suggest that designers of mobile devices need to take them into account.

The first experiment was designed to determine the subjective equivalence of vibration magnitude for devices having different weights. While manipulating several mobile devices of varying weights, it was observed that the perceived vibration strength varied for the *same* measured acceleration magnitudes. The existence of a weight-vibration perceptual interaction can then be hypothesized from the results of a pilot experiment [138]. In the present article, an improved experiment is described in Section 5.

A second experiment was motivated by the trend seen in the industry to use higher vibration frequencies. This is a result of using the peak-to-peak acceleration as the only measurement of vibration strength and not considering the underlying driving frequency.

As the phone size decreases, designers choose smaller motors that can achieve the same magnitude levels by spinning at a faster rate. To establish the relationship between perceived vibration strength and frequency, a magnitude matching test was performed targeting the conditions found for typical mobile devices. It was expected that the results would generally agree with those of previous studies indicating that higher frequencies require higher accelerations to achieve the same perceived strength.

5.4 Experimental Setup

Mock cellphone devices were manufactured with weights and sizes similar to that of common portable phones. Each contained a high-bandwidth actuator and an accelerometer mounted on the outside casing of the device. The method of adjustment was used whereby participants adjusted the vibrating strength of a given mock phone to match that of a reference device.

5.4.1 Apparatus

Four mock cellphones were fabricated (84 × 55 × 20 mm), along with their controlling circuitry. The devices weighed 50, 110, 110 and 200 g. The second 110 g device served as the reference and was used to assess how well subjects could match identical devices. Each contained a custom-made, recoil-type Lorentz actuator made of a magnet suspended inside a pair of coils in an open magnetic circuit arrangement [119]. It could accelerate a 110 g box up to 30 m/s^2 from 70 to 500 Hz with minimal distortion. The vibration strength could be adjusted by turning a rotary control similar to that of audio equipment. Each had a software-calibrated accelerometer (MMA7260Q, Freescale) to capture the individual device acceleration.

The controlling circuitry consisted of a microcontroller board (LPC2148, Phillips), a 12-bit digital-to-analog converter (DAC7616UB, Texas Instruments) and a 7 W audio amplifier (LM4752T, National Semiconductor). The microcontroller read the acceleration with the internal 10-bit analog-to-digital converters at 3 kHz. It communicated with the computer via serial port at 11.5 kb/s for the values of accelerations captured during the experiments. It also synthesized output signals for the digital-to-analog converter at 15 kHz, which was connected to the amplifier of the actuator.

5.4.2 Method

Both experiments used the method of adjustment to evaluate the equivalent perceived strength under different conditions. This method has the distinct advantage of requiring shorter experimental duration than the method of constant stimuli. This advantage is particularly important given the well-known sensory adaptation of vibrations in the sense of touch [139, 140]. Moreover, the vibration signal was targeted at levels that are known in the industry to be suitable for capturing the attention of users. Because of the higher values used in this study, it was critical that the duration of each experiment was not too long to avoid fatigue and boredom. For these reasons, it is also the method of choice in most studies concerning vibrotactile perception, e.g. [66, 53].

5.5 Experiment I: Weight

The goal of this experiment was to determine the subjective equivalence of vibration strength for devices of three different weights, similar to the 2007 study [138]. This experiment differed from the 2007 study in that:

- The mock telephones were slightly larger: 84 × 55 × 20 mm instead of 80 × 40 × 17 mm.
- The accelerations were now half as low: 0.67-2.5 m/s^2 r.m.s;
- Each point in the figure was the average of two trials, with one very low and one very high initial vibration strength.
- The r.m.s values were now obtained directly from the recorded signal instead of being filtered before calculation. This yielded a more consistent measurement of the reference acceleration.

5.5.1 Stimulus

Sinusoidal vibrations of 150 Hz with amplitudes from 0.67 to 2.5 m/s^2 r.m.s, or 2 to 7 m/s^2 peak-to-peak, were used. The signals were pulsed at 1 Hz in a 500 ms-on, 500 ms-off manner to simulate signals from a real mobile phone. For each participant, the experiment consisted of 18 trials. For each acceleration and weight, two trials were performed with the

initial signal strength set to very low and very high. The trial sequence of the experiment was randomized for each participant.

5.5.2 Procedure

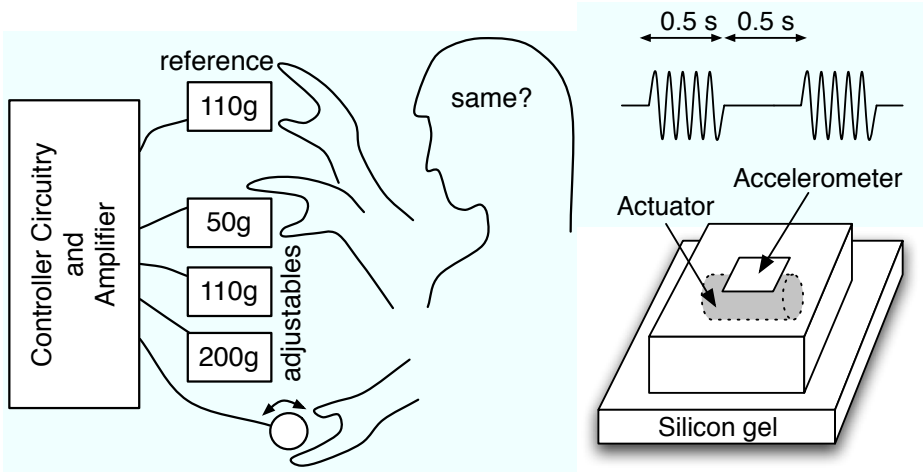

Fig. 5.1 Experimental Setup

Twelve healthy subjects (4 males, 8 females) participated in this experiment. They were all university students or staff, aged from 18 to 35, each paid for their time. All reported having personal experience with mobile devices. They wore sound-isolating headphones (rated 12.2 dB attenuation at 125 Hz) playing white noise to eliminate the influence of sound during the experiment.

During each session, the participant was seated in front of the four devices. The devices were resting on blocks of silicone gel with similar mechanical characteristics as the hand. The participant used the dominant hand to manipulate the device and the other hand to control the vibration strength via a rotary control. There was one reference device, R, and 3 adjustable devices, A_1, A_2 and A_3. For each trial, device R and one of the adjustable device, A_x, would vibrate. The participant then had to pick up the device, assess the vibration strength, and then adjust the strength of the device A_x until its vibration was perceived as having the same strength as the reference device R. When the participant was done, she or he placed the device back on the gel block and signaled the tester to proceed to the next trial. This allowed a careful acceleration measurement independent of the user's grip and device orientation. The acceleration of each device was recorded and logged by

computer before the next trial.

All participants completed the experiment within 25 minutes. The procedure was approved by the Research Ethics Board of McGill University.

There is one important remark to be made regarding the condition under which the acceleration was measured. The measured acceleration is proportional to the mechanical energy input, but the energy absorbed by the touched object cannot be directly obtained from this measurement. When the device is held by a hand, if the signal strength increases, the absorbed vibration increases as well. At the same time, a stronger signal requires a larger grip force, which also interferes with the vibration absorption characteristics [141]. The change of hand impedance makes it difficult to make measurements when the device is held in the hand, therefore the acceleration was measured under a controlled condition on a silicon pad.

5.5.3 Results

The results suggest that a larger weight requires less acceleration to produce the same perceived strength, which is consistent with our previous study [138]. The measured accelerations for each weight are fitted to straight lines, as plotted in Fig. 5.2. The results from one participant were excluded from the analysis due to a clear difference compared to the rest of the group. The logarithmic relationship used in Fig. 5.2 is employed to explain many aspects of perception such as vision, weight or sound, and can be described by the Stevens' power law. Some studies have used *decibels* to measure intensity level, which is defined as ten times the logarithmic of the power ratio. Here, the *decibel* is not a suitable unit as the power ratio for different frequencies cannot be directly related to the measured acceleration. To keep data manipulation to a minimum, we have chosen to simply use log(acceleration) in the analysis.

The analysis of variance (Friedman) gives $p<0.001$ when the data were in pairs and for all (χ^2=62.24, df=2), showing significant differences among the three groups. Each point in the figure is the average of two trials, with one low and one high initial vibration strength. The analysis of variance shows no significant difference between the two initial strengths (p=0.1511);

The values of the slopes are: $k_{50g} = 0.93$, $k_{110g} = 0.90$, $k_{200g} = 0.67$, again similar to our previous results. The lower slope found for 200 g is due to the larger variability in the measurement of the lower acceleration values. This variability is mainly caused

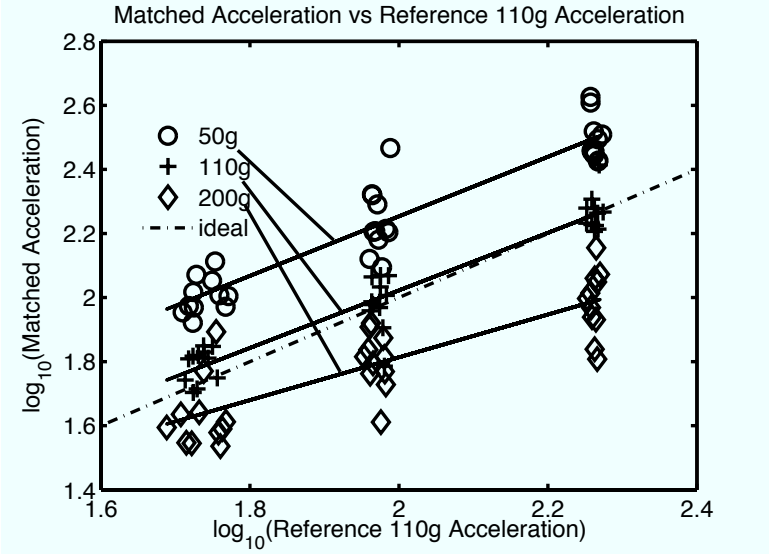

Fig. 5.2 Adjusted acceleration versus the reference acceleration.

by limitations from the sensor and the acquisition system. The accelerometer produces an output voltage of 40 mV for 2 m/s^2 (0.2G). It has a r.m.s. noise of 4.7 mV, which, combined with the 3.2 mV precision of the analog-to-digital converter, results in around 8 mV of precision in total. We believe that this limitation does not make measurements of 40 mV invalid, but contributes to the spread in the calculated r.m.s. values. Notice that such a spread is not present for higher acceleration.

To compare the data from the 2007 and 2009 experiments, the values of the relative perceived strength are plotted side-by-side in Fig. 5.3. The present study shows a clearer separation of the three different weights. Despite the different acceleration range, the mean values of the relative perceived strength for each weight remain very similar.

One important law describing the relationship between the physical stimulus magnitude and the perceived strength is Stevens' power law, $\Psi(I) = kI^a$, where I is the stimulus magnitude (weight), $\Psi(I)$ the perceived strength, k the proportionality constant, and a the exponent that depends on the type of stimulation. Assuming this relationship true in this case, the relative perceived strength from each of the experiments, as well as both combined, can be converted to logarithmic and fitted to a linear polynomial $\log(\Psi(I)) = a * \log(I) + \log(k)$, or in the format $f(x) = ax + b$, as shown in Fig. 5.3. The resulting lines are all within the 95% confidence bounds of each other.

Notice that all three lines cross very close to the (110, 0) point, meaning that the

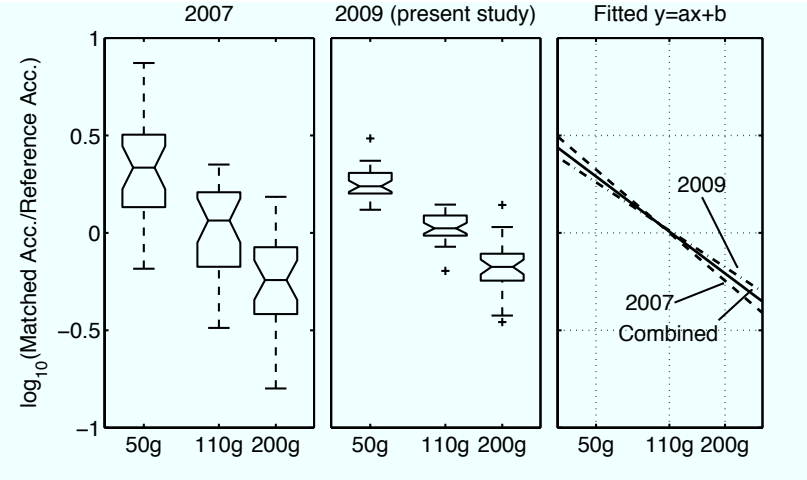

Fig. 5.3 Box plots showing the relative perceived strength for the previous experiment (2007) and the present one (2009), as well as the fitted lines. The horizontal axis follows the logarithmic scale.

Table 5.1 Values in $f(x) = ax + b$ and correlation coefficients r^2

Data Set	**a**	**b**	r^2
Experiment 2007	-0.4118	1.936	0.499
Experiment 2009	-0.3143	1.489	0.792
Combined	-0.3590	1.694	0.577

vibration strength of two equally weighted boxes were perceived the same.

5.5.4 Discussion

The results confirm the findings from our past study that the heavier the box, the lower the r.m.s. acceleration required to produce the same perceptual strength. This relationship is sufficiently clear-cut to be quantified and fitted into a linear polynomial.

Our findings have several important practical implications. With today's phones containing more sophisticated haptic capabilities, it is important to understand how the physical properties as well as the tactile patterns chosen for applications are perceived by the user. Great time and energy is spent by cell phone manufacturers to ensure the look and feel of the mobile phone is ergonomically pleasant. This should extend as well to the haptic capabilities of phones. To ensure high quality and consistent haptic effects, whether for attention or communication, across multiple models, the device weight needs to be factored into the haptic design process as it directly impacts the user's perception of vibration strength. With the quantitative knowledge given in Table 1, designers can account for the varying weight of handheld devices at design time, or compensate automatically for the weight of the device in the haptic controller.

The stimuli impinging our senses often requires cognition to be related to the real world. During the experiment, the participants manipulated the devices freely and it was noticed they did not hold the device statically: they turned the device in their hand, varied the grip force and position, and alternated between the reference and adjustable boxes by picking them up and putting them down. The contact area of the skin, the mechanical impedance of the hand and the mechanical energy absorbed were likely to vary during these activities. Regardless of how one manipulates the device, the perception of the physical characteristics of the device remained unchanged. This perception of constancy cannot be explained only by the contact area of the skin or the muscle activities. One way of increasing contact area and absorbed energy [141] is to increase the grip force, but it does not change the perception of vibration strength in a consistent way [57]. This phenomenon is similar to the constancy effect observed when the same object is probed with a tool held with different grips [142].

The energy absorbed by the hand changed dynamically during the experiment, and there is no easy way to measure or even estimate it without carefully examining the mechanical impedance of the hand-arm system. Nevertheless, it is remarkable that our perception

system is able to combine all the sensory inputs under different conditions to produce a stable estimation.

5.6 Experiment II: Frequency

The goal of this experiment was to determine the subjective equivalence of vibration strength for frequencies from 80 to 220 Hz.

5.6.1 Stimulus

In this experiment, two mock cellphones were used, both weighing 110 g. The reference device R was driven at 150 Hz with acceleration around 2.5 m/s^2 r.m.s., (7 m/s^2 peak-to-peak), and the adjustable device A was driven at a frequency ranging from 80 to 220 Hz. Both devices were driven with a pulsed signal at 1 Hz with 50% duty cycle. The amplitude of device A could be changed using a rotary dial, whereas the amplitude of R remained the same throughout the experiment. The experiment sequence, as well as the initial strength, was randomized for each participant. There were 15 trials in total for 80 to 220 Hz with 10 Hz intervals.

5.6.2 Procedure

Eleven (11) university students and Immersion employees participated in the experiment. The participants all wore headphones playing white noise to minimize the effect of sound during the experiment. While seated, the dominant hand was used to handle the devices while the other hand controlled the vibration strength of device A via a rotary control. For each test case, the participant was instructed to tune the vibration strength of the device A such that it had the same strength as the device R. When the participant was done, she or he placed the devices on blocks of silicone gel having similar viscoelastic characteristics as those of the human hand, and signaled the tester to proceed to the next test. Device A changed its underlying drive frequency for each trial case, but not R. The experiment lasted approximately 15 minutes for each participant.

5.6.3 Results

The experimental results suggest that the higher the driving frequency, the higher r.m.s. acceleration value is necessary to produce the same perceived strength.

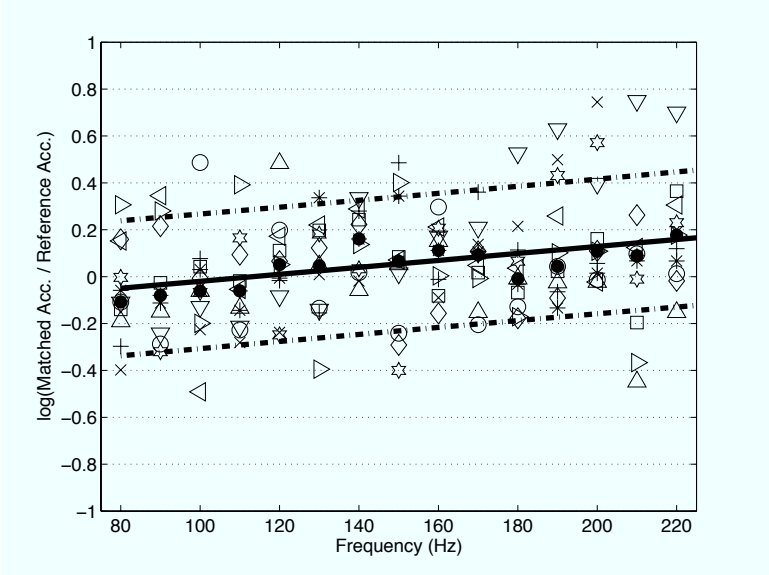

Fig. 5.4 Adjusted acceleration versus the reference, with the solid fitted line and dotted lines covering 80% of data. Each symbol represents one participant, and the medium values are the filled dots.

Fig. 5.4 plots the results of all the participants, as well as the fitted line with 80% data bounds. The slope of the line is 0.0018 (95% interval of confidence [0.001006, 0.002615], r^2=0.10). Unlike Experiment I, the horizontal axis follows a linear scale instead of logarithmic. The logarithmic function for this narrow frequency range is nearly linear; therefore to keep data manipulation to a minimum, the linear scale is chosen here. Despite the poor fit indicated by the correlation coefficient r^2, the positive slope of the fitted line (interval of confidence not including 0) suggests that the frequency influences the perceived vibration strength.

To verify if the results for each frequency are significantly different, an analysis of variance test (Friedman) is performed. The result ($p<0.01$, χ^2=30.01, df=14) suggest a statistically significant difference among the frequencies despite the scatter. A closer look shows that the data from neighboring frequencies are very similar, but not when they are far apart. For example, the results for the frequency, 80 Hz are significantly different from the ones for 220 Hz; however, the results for 150 Hz are not significantly different from all

other frequencies.

The observed tendency is that when the frequency is lower, the perceived strength is lower than the corresponding acceleration, whereas in higher frequency, it is the opposite. This tendency is statistically significant, despite the relatively narrow range tested, which is a little more than one octave. The fitted line crosses the reference 150 Hz at a small positive value, but the (150,0) point is well enclosed within the interval of confidence.

Due to the large variability and the narrow range of frequencies, this experiment does not provide data sufficiently reliable to establish an equal sensation contour.

5.6.4 Discussion

The positive slope of the fitted line in Figure 5.4 suggests that the higher the underlying frequency, the greater r.m.s. acceleration is needed to produce the same perceptual magnitude. This is consistent with our hypothesis, as well as existing literature for continuous vibrotactile signals on grounded devices. A good example of such a study is provided by Morioka and Griffin, where the equivalent comfort contours for above-threshold continuous vibration on steering wheels was established [59]. The fact that mobile devices are not mechanically grounded and that they give pulsed signals does not seem to change the overall perception tendency.

Experiment II was also designed to focus on the frequencies between 80 and 220 Hz, a range relevant for mobile devices. The large variability in the results suggests that it may not be necessary to probe at intervals as close as 10 Hz for this frequency range. It has been reported that the limit of human capacity for frequency discrimination is around 20-40 Hz for continuous signals on hairy and glabrous skin in this range[70].

Compared to other studies [59], the slope of the matched value with respect to frequency in Figure 5.4 is less steep for the same frequency and acceleration. One likely reason is the pulsing scheme of the signal. When the signal is pulsing at 500 ms on, 500 ms off fashion, the total energy output is 50% smaller than what would be when the signal is continuous. This put the equivalent signal strength from 2.5 down to around 1.3 m/s^2 r.m.s. For this acceleration value, the slope is in fact less steep. It is hard to quantify and compare the slope because of the wide range of variance in the data.

5.7 General Discussion

The first experiment examines how the weight of a mobile device influences the perception of its vibration signal. Using acceleration as the measurement unit for vibration, heavier devices create a positive offset in the perceptual strength. The second experiment suggests that the perceived strength decreases as the frequency increases.

The outcome from the first experiment strongly indicates the need for further studies on how different aspects of tactile perception interfere with each other. Acceleration, which unlike force unambiguously describe the physics of a vibrating object, is only one of the factors that can be used to quantify the perceptual outcome of vibratory stimuli in mobile devices.

The outcome of the second experiment confirms our hypothesis and corresponded to results from past studies. Similar studies, on grounded devices, have been done with the finger pad, whole hand pressing on a vibrating plate, hand holding a vibrating handle, as well as on different parts of the human body. The signals used ranged from sub-threshold, < 0.005 m/s^2 to supra-threshold values, > 30 m/s^2. Depending on the signal strength and frequency, most authors suggested that the perception pattern is shaped either by different kinds of mechanoreceptors or the mechanical impedance of the skin and bone structure. Holding a mobile device, as compared to holding a grounded device, activates a different set of motor activities and sensory inputs; however, it does not seem to interfere with the mechanism responsible for vibrotactile perception for different frequencies.

5.7.1 Design Recommendation

In the design of mobile devices, size and energy consumption are among the most important constraints. As designers squeeze more electronics inside smaller volumes, the mechanical counterparts, such as vibration motors, are also required to be reduced in size.

Haptic specifications for older model phones generally consisted of the need to meet a minimum vibration level. One way designers addressed the required specifications of smaller motors, and hence smaller driven masses, was to increase the frequency of the motor. This allowed them to meet the requirements, however as the results in this study show, the overall perceived strength is affected by both the weight of the device and the underlying driving frequency. These factors, as well as the dynamic properties of the actuator, need to be considered when developing haptic systems with rich content that have the ability

to convey a wide range of information to a user. It also becomes important to develop tools that allow designers and manufacturers to create consistent haptic effects across their platforms and applications.

While cellphone related technologies have progressed at a remarkable speed, little has been done on haptic perception relevant to mobile devices. The work presented here demonstrates the need for further research on how different aspects of physical and signal property interfere with the perceived strength.

5.8 Conclusion

This paper describes experiments studying two factors that influence perceived vibration strength in mobile device: weight and vibrating frequency. Given the same surface acceleration, the results showed that the heavier the device, the stronger the perceived strength. The results also confirmed that the higher the driving frequency, the weaker the perceived strength. Both experiments obtained similar conclusion to past studies of vibration perception under different conditions.

Many other factors remain to be examined in vibrotactile perception with mobile devices. For example, the vibration pattern used in this study was a 500 ms on, 500 ms off condition. Today's cell phones with advanced haptic capabilities use more complex vibration patterns and pulses as short as 5 milliseconds. The influence of different patterns on attention grabbing, magnitude perception and pleasantness needs to be further examined. Furthermore, in much of the existing literature, vibration is treated as unwanted, background noise. In the case of a haptic enabled cell phone, vibration is used as a private channel to convey information to the user. The vibration patterns should be as noticeable and informative as possible, while remaining discreet and pleasant.

Acknowledgment

This study is jointly funded by Natural Sciences and Engineering Research Council of Canada and Immersion Corp. The authors would like to thank Immersion Corp. for initializing the study, Dr. Vincent Hayward for his insightful comments and Dr. Ilja Frissen for help on experiment design and analysis.

Chapter 6

Simulation of a Rolling or Sliding Object

One of the ultimate goals in the advancement of haptic devices is to be able to re-create the real world tactile experience in simulation. There would be two benefits from achieving this goal: first, the more realistic the simulation is, the more we can be confident that our understanding of tactile perception is accurate; second, a realistic simulation provides a tool to manipulate the sensory stimulus in a way that was impossible to achieve with real-world objects, yet essential for a better understanding on how perception works.

The natural phenomenon that sparked this study is the vibration felt when holding a tube with an object moving inside. The following manuscript aims to study if and how humans can estimate the traveled distance of the object by tilting and feeling the rolling vibration. With access to the tilt angle and haptic signal, the pilot study showed that most people are able to give an estimate on how far the object has traveled. The apparatus in this experiment also used the high-bandwidth, light-weight actuator presented earlier. The realism was such that most participants in the experiment believed there was a real ball inside.

This article appeared in *Proceedings of EuroHaptics 2006*. The demonstration of the device in the conference also received the *Best Hands-on Demo* voted by the conference delegates.

An Experiment on Length Perception with a Virtual Rolling Stone

by Hsin-Yun Yao and Vincent Hayward

Abstract

When an object rolls or slides inside a hand-held tube, a variety of cues are normally available to estimate its location inside the cavity. These cues are related to the dynamics of an object subjected to the laws of physics such as gravity and friction. This may be viewed as a form of sensorimotor coupling which does not involve vision but which links motor output to acoustic and tactile inputs. The theory of sensorimotor contingency posits that humans exploit invariants about the physics of their environment and about their own sensorimotor apparatus to develop the perception of the outside world. We report on the design and the results of an experiment where subjects held an apparatus that simulated the physics of an object rolling or sliding inside a tubular cavity. The apparatus synthesized simple haptic cues resulting from rolling noise or impact on internal walls. Given these cues, subjects were asked to discriminate between the lengths of different virtual tubes. The subjects were not trained at the task and had to make judgments from a single gesture. The results support the idea that the subjects mastered invariants related to the dynamics of objects under the influence of gravity that they were able to use them to perceive the length of invisible cavities.

6.1 Introduction

The experiment described in this paper was inspired by the ball catching experiments of McIntyre et al. and Senot et al. [101, 143]. They showed that subjects exposed to a variety of distortions of sensory inputs including the removal of gravity, or the up-down inversion of their retinal image, maintained a surprisingly robust, pre-establish notion of gravity that was manifest in their anticipatory motor behavior. We were also inspired by the work of Lenay et al. who attached a photo detector and a vibrotactile stimulator to one finger of blindfolded subjects and placed a bright point light source in their vicinity [144]. The system was so rigged that when the photo detector was pointing in the direction of the light source, the subjects experienced a single-pulse vibrotactile sensation. The authors report that during free exploration, typically, subjects progressively developed the perception of a distal, exterior object, that is, one which was not in contact with the skin.

O'Regan and Noe's theory of sensorimotor contingency provides us with a framework to investigate this type of phenomena [93]. A simplified account of this theory holds that perception arises when an organism discovers pre-existing invariants about the world and about itself and learns how to use them, something the authors call a *sensorimotor law* [145, 146]. In Lenay's experiment, the invariant was determined by the geometry of the propagation of light and by the *sensorimotor coupling device*, the properties of both of which were *a priori* unknown to the subject. It is easy to show that only one location of the source could explain a highly reliable correlation between specific finger pointing directions and the occurrence of a tactile pulse, hence the "exteriorization" of the stimulus as anticipated by Katz (see [79], "vibration has many of the capabilities of a far sense"). Robles-De-La-Torre and Sekuler showed that people could rapidly discover dynamic invariants, despite the presence of an abstract and highly impoverished sensorimotor coupling [147].

In McIntyre's et al. experiments, gravity participated in the invariant behind the sensorimotor law linking visual input to hand movement, and eventually to the sensation of the ball hitting the hand. It is natural that learned gravity-related invariance in humans (and probably in most animals) be extraordinarily resilient to drastic perturbations of the sensorimotor couplings given the pervasiveness of gravity from the day we are born. It is also critical for survival that gravity and associated invariants be precisely established.

6.2 An Interesting sensorimotor Task

It will be easier for the reader to understand our experiment if she is kind enough to get hold of a tube, to place a small round object inside it and close the ends. It could be something as small as a drinking straw with a rice grain inside, but a cardboard tube to transport posters with a small wood, rubber, or metal ball will be more compelling. The reader can then appreciate how effortlessly she can predict the instant of collision between the ball and the cap. This is especially true if the eyes are kept open, although vision provides information about the tube but not about the object. Since the moving ball is not seen, predicting its collision entails estimating its position at all times. This requires solving its equation of motion from known initial conditions.

Since Galileo, we know that a ball rolling down a ramp inclined by angle $\alpha(t)$ travels a distance

$$d \approx d_0 + k \iint_0^T \sin \alpha(t)\, dt^2. \tag{6.1}$$

This expression is independent from the mass of the objet if we ignore losses and neglect the acceleration due to the change of angle. Two cases arise in the experiment just described.

Either the subject has access to d_{cavity}, the length of the cavity, say by seeing and touching the tube (which is another thorny sensory motor problem! Let's assume this problem to be solved), and the subject must solve the above equation for T to predict the collision. Evidently, the problem is simplified if the subject keeps the tube at a constant inclination, in which case there is a simple expression for T. The task corresponds to the solution of an inverse problem, provided that k was known from another inverse problem.

A second experimental condition is created when the distance d_{cavity} is unknown from the subject, for example if an experimenter placed invisible walls inside the tube to limit the travel of the ball. The task is then to guess the distance over which the object is limited to travel. This is feasible only if the subject can solve a direct problem where the unknown is d_{cavity} as well as an inverse problem for k. It is the case that we investigate in this paper because testing subjects is simple since the task is to guess the rolling length.

6.3 A More Detailed Analysis

6.3.1 Physics

The constant k in Eq. (6.1) takes specific values according to the mass distribution of the rolling object. Write $L = mgh + \frac{1}{2}m\dot{x}^2 + \frac{1}{2}I\dot{\theta}^2$, where x, θ, and h are the position, angle, and height of the object, m and I are its mass and moment of inertia, and g is the intensity of the gravity field. If r is the rolling radius then $dx = r\,d\theta$, and Lagrange's equation gives $k = g/[1 + I/(mr^2)]$. Without learning, this can make the sensorimotor tasks described in the previous section very difficulty indeed. For instance, Figure 6.1a shows a rolling object designed to have a malicious behavior. The rolling radius r is such that $I/(mr^2)$ is a number much greater than 1. On the other hand, the case of solid ball, Figure 6.1b, is such that $1 + I/(mr^2) = 1.4$ since $I_{\text{ball}} = \frac{2}{5}mr^2$. This case is admittedly very common to us (marbles, pinball machines, and golf balls) and is, again, invariant with mass. Later in our simulations, we will make a virtual rolling ball obey:

$$\ddot{x} = \frac{g}{1.4}\sin(\alpha(t)) \approx 7.0\sin(\alpha(t)). \tag{6.2}$$

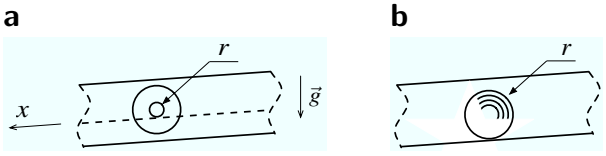

Fig. 6.1 **a**) Unusual case. **b**) Usual case.

Another case of related interest is that of an object sliding down the tube. Assuming that both Coulomb's and Amonton's laws are good enough to apply, if μ is the coefficient of friction between the two sliding surfaces, then the object's motion is governed by

$$\ddot{x} = \begin{cases} g[\sin(\alpha(t)) - \mu\,\text{sgn}(\dot{x})\cos(\alpha(t))], & \text{if } \tan(\alpha(t)) > \mu \\ 0 & \text{otherwise.} \end{cases} \tag{6.3}$$

This is still invariant with mass but now at least one additional unknown quantity, μ, participates in the resulting displacement of the invisible object. Without prior knowledge this makes the task of finding the sliding length more difficult.

6.3.2 Cues

During tasks with a ball rolling inside a tube, a variety of acoustic and haptic cues are available to the subject. First, rolling causes the tube to vibrate, yet not periodically since the ball's velocity is generally not constant. The pseudo-period of the vibration, or its spectrum, which can be felt and heard, is related to the ball's velocity. But velocity cannot be directly observed given the many unknown factors contributing to the signal. Nevertheless, it is plausible that this signal can be processed to estimate the change of velocity, i.e. the acceleration, by autocorrelation in the time domain or by spectral shift estimation. A second basic cue is the plain duration of the roll which is also a bimodal cue. A third bimodal cue is the intensity of the impact felt when the ball hits the wall. The energy dissipated by an inelastic collision is $E_{\text{loss}} = \frac{1}{2}mv_a^2(1 - e^2)$, where v_a is the approach velocity of the ball just before it hits the wall and e the coefficient of restitution. The product $\frac{1}{2}m(1 - e^2)$ is another invariant that may be estimated after several trials to eventually give access to v_a from which d can deduced. A fourth cue that is purely haptic is the transfer of weight caused by the movement of the ball. It can be subtle or prominent according to the relative masses of the tube and the ball. Other monomodal or bimodal cues probably exist, such as the intensity of the vibration growing with the ball's velocity, that are probably exploited during the tasks described. For the case of an object sliding without rolling, access to the change of velocity through spectral shift no longer is available or in a greatly weakened form, but the other three cues remain.

In all cases, subjects must have also access to the angle $\alpha(t)$. Interestingly, it is likely that they can estimate it from at least four distinct sources of information. The first are motor commands issued to incline the tube at a desired angle, the second are proprioceptive cues arising from the posture of the entire body, including limbs and extremities, the third are visual cues allowing the subject to compare the viewed tube with surrounding structures, and the fourth is the static loading caused by the tube which may be picked up proprioceptively or cutaneously and which is proportional to $\cos(\alpha(t))$. It is also plausible that vestibular cues participate in reporting the direction of the ambient gravity field.

A related case of particular relevance is when the velocity of the ball is proportional to $\sin(\alpha(t))$ instead of its integral. This actually happens with a musical percussion instrument called the "rain stick". It is a dried, hollowed branch of a cactus in which many horns grow across the inner compartment along many diameters. The inner maze cause pebbles that have been placed inside to descend in a "pachinko game" fashion, the many collisions

causing their *average* velocity to be low and steady (resulting in a steady rain-like sound). This is highly relevant to the foregoing discussion because a very first encounter with the instrument typically results in wonder and amazement owing to the fact that the vibrations emanating from the tube grossly violate the invariance rules that we have outlined earlier.

6.4 Experimental Approach & Question

The abundance of cues available to a subject wielding a tube containing a ball or a sliding object makes it hard to design well controlled experiments, but by employing haptic technology, it is possible to reproduce the essential aspects of the tube and ball dynamics, while having freedom in the construction of desired sensorimotor couplings.

An apparatus, Figure 6.2, was constructed by inserting a powerful electromagnetic recoil actuator and an accelerometer inside a tube. These elements were connected to a microprocessor. This way, we could create any type of sensory feedback, haptic or acoustic, in response to the movement of the tube with respect to the ambient gravity field.

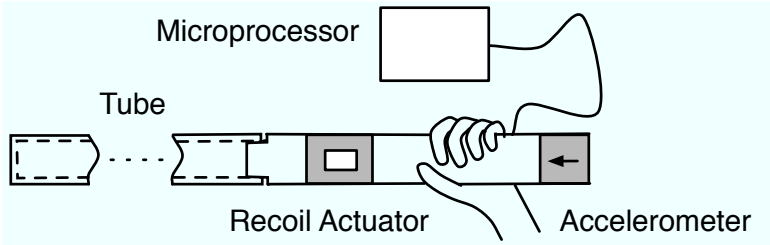

Fig. 6.2 System simulating an object sliding or rolling

To good approximation, it is possible to make this apparatus behave like a tube containing an object by simulating the physical principles set forth in the previous section and by programming it to produce desired sensory cues. It is also possible to endow the device with nonphysical behaviors such as objects having unusual inertial behaviors, to decouple the haptic response from the acoustic response, to add or remove dry friction, viscous friction, etc., etc., (including making it behave like a rain stick).

In the present study, we restricted ourselves to imitating the ordinary response of a ball rolling or sliding in a tube under the normal gravity field but without transfer of weight. We asked the subjects to handle the tube within shallow angles only, lest they suspect something abnormal at steep angles where a real ball would no longer roll but slide or

free-fall. Also, they could not hear the sound it produced, but they could see the tube normally.

We hypothesized that under these conditions, naive subjects *without any kind of practical or theoretical training*, could use either the balling-rolling-rumble cue, or the time-to-collision cue, as sole source of information in a spontaneous, one-shot, length estimation task. From the above discussion, the task was feasible only if the rolling ball or sliding object invariants were available to the subjects before the trials.

6.5 Methods

6.5.1 Apparatus

The apparatus comprised a 60 cm-long, 1.3 cm diameter fiber-glass tube which weighted about 300 g, and a sensor/actuator subassembly unit rigidly attached to the tube. This unit was connected to a custom-made, single-board microprocessor subsystem, see Figure 6.2.

An accelerometer (Model ADXL210, Analog Devices, Norwood, MA), gave readings that were acquired by the microprocessor (MSP4301612, Texas Instrument, Dallas, TX). An on-chip 12-bit digital-to-analog converter drove an audio amplifier that powered a custom-made actuator. It had a magnet suspended by two membranes inside a pair of coils, see Figure 6.3. The geometry was such that current generated a Lorentz force between the magnet and the coils. By conservation of momentum, acceleration of the magnet was matched by acceleration of the case held by the subject.

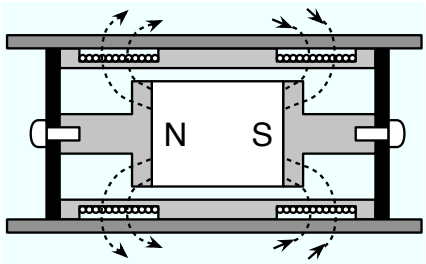

Fig. 6.3 The Actuator.

The weight of the sensor and of the actuator was such that the apparatus felt like an ordinary hollow tube. It had the visual appearance depicted by Figure 6.4. The beginning of the hollow section was indicated by the visible connection between the sensor/actuator unit and the tube.

Fig. 6.4 Apparatus used in the experiment.

The microprocessor ran software to simulate the key aspects of the physics discussed earlier and generated specific cues, thus creating desired sensorimotor couplings. The accelerometer measured the component of the acceleration vector that was in the direction aligned with the main axis of the tube and rejected the others. What the accelerometer measured was the acceleration of a frictionless point mass that would be located where the measurement was made. In the apparatus, the virtual object moved but the accelerometer was fixed with respect to the tube. Provided that the subjects subjected the apparatus to movements that were sufficiently slow, to good approximation the sensor returned a measurement directly proportional to $g \sin(\alpha(t))$.

For the case of the simulation of a rolling ball, the software solved a finite difference version of Eq. (6.2) using the trapezoidal integration rule, and reset $\dot{x}$ to zero whenever d met one of the two ends of the virtual tube.

$$
\begin{aligned}
\ddot{x}_k &= 7.0\, sin(\alpha_k), && \ddot{x} \text{ directly from the sensor,} \\
\dot{x}_k &= \begin{cases} 0 & \text{if } (x_{k-1} < 0) \vee (x_{k-1} > d_{\text{cavity}}), \\ \dot{x}_{k-1} + h\dfrac{\ddot{x}_{k-1} + \ddot{x}_k}{2}, & \text{otherwise} \end{cases} \\
x_k &= x_{k-1} + h\frac{\dot{x}_{k-1} + \dot{x}_k}{2},
\end{aligned}
$$

where the system's sampling period was $h = 1/256$ s.

To synthesize rolling noise, an "artificial source-natural filter" approach was adopted. The source waveform was generated by repeating the positive arch of a sine wave. This waveform has a strong fundamental component and both even and odd harmonics. The filter was simply the natural dynamics of the actuator and the tube. Thirty samples of the sinusoidal arch were stored in a "wavetable" that was looked up by the index $i = x_k \bmod 30$. This way, if x_k was expressed in millimeters, the waveform repeated itself every 30 mm,

which corresponded to a ball of about 1 cm diameter. Figure 6.5a shows the spectrogram of the generated source waveform when the virtual ball was made to roll at an inclination of 27°, and Figure 6.5b shows the resulting measured acceleration. Figure 6.5a clearly shows the linear increase in velocity of the virtual ball and the corresponding shift of the spectrum linearly with time. Figure 6.5b shows the filtered version of the signal where the actuator's natural resonance (see Figure 6.6) enhanced the 100 Hz band and where the multiple violations of the Nyquist's condition created much high frequency noise. This resulted in a plausible rolling noise that was partly deterministic and partly stochastic.

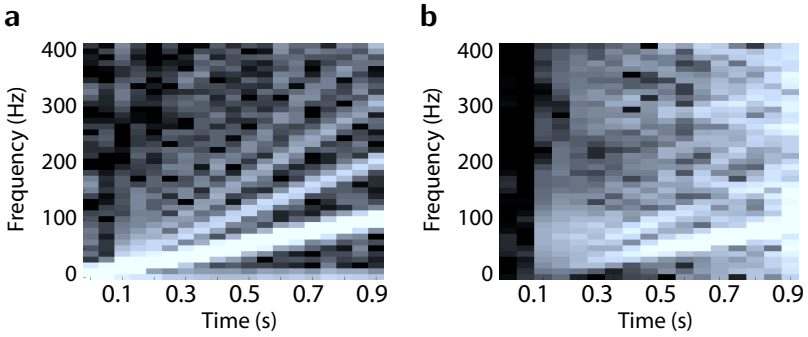

Fig. 6.5 **a**) Spectrogram of source signal. **b**) Spectrogram of the filtered recorded acceleration.

For the case of an object sliding down the tube, the microprocessor solved a finite difference version of Eq (6.3) by the trapezoidal rule also. Approximating g by 9.8, assuming $\mu = 0.2$, and replacing the sign of the velocity by the sign of the inclination angle to avoid spurious switching, we had:

$$\ddot{x}_k = \begin{cases} 0, & \text{if } \sin(\alpha_k)^2 < 0.2(1-\sin(\alpha_k)^2) \\ 9.8\,\sin(\alpha_k) - 1.96\,\operatorname{sgn}(\sin(\alpha_k))\sqrt{1-\sin(\alpha_k)^2}, & \text{otherwise} \end{cases}$$

$$\dot{x}_k = \begin{cases} 0, & \text{if } (x_{k-1} < 0) \vee (x_{k-1} > d_{\text{cavity}}), \\ \dot{x}_{k-1} + h\dfrac{\ddot{x}_{k-1} + \ddot{x}_k}{2}, & \text{otherwise} \end{cases}$$

$$x_k = x_{k-1} + h\frac{\dot{x}_{k-1} + \dot{x}_k}{2}.$$

To synthesize the impact of an object hitting the end of the tube, we set the actuator signal at a fixed amplitude during one sample period and made the amplitude of the pulse

proportional to the virtual impact velocity. This way, the energy dissipated in the hand of the subject was directly proportional to the square of the virtual impact velocity which was consistent with the physics of an impact as seen earlier. The sensor/actuator unit was housed in a 10 cm tube section that was attached to a 60 cm extension. Recordings were made when the sensor/actuator unit was disconnected from the tube and when it was attached to it. The results are reported in Figure 6.6 where the 100 Hz natural resonance of the actuator can be noticed as well as the attenuation brought by the heavier tube. During preliminary trials with several volunteers, we found this response realistic enough.

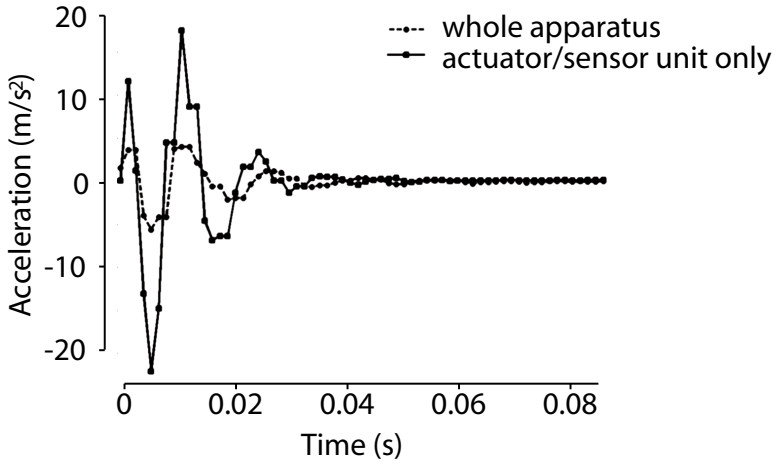

Fig. 6.6 Impulse Responses with tube attached or removed.

We validated the simulation by measuring the time required for a real irregular ball to travel 60 cm on an inclined surface and did the same with the apparatus. The measurements were made 12 times for a 10° inclination and again 12 times for 30°. Table 6.1 summarizes the results for each case.

Table 6.1 Mean rolling durations, real and virtual.

	10°	30°
Real	0.9987 s, $\sigma = 0.1458$	0.4512 s, $\sigma = 0.0999$
Simulation	1.1354 s, $\sigma = 0.1304$	0.4082 s, $\sigma = 0.0125$

6.5.2 Procedure and Subjects

Eight students from McGill University's Electrical and Computer Engineering department kindly volunteered for the study. They were asked to guess the length of the tube by tilting it and experiencing the hidden object's dynamics. To avoid any possibility of learning, the subjects were divided in two groups. Four subjects experienced only the rolling noise cue produced by simulating the rolling dynamics and there was no simulated impact as if the tube had soft internal walls. Four other subjects experienced the impact cue only by simulating the sliding dynamics, but did not experience the rolling noise cue as if the object slid very smoothly.

All subjects were told that there were three inner tubes inside the apparatus. Two were short: 18 cm and 24 cm in length, and one was long: 60 cm in length. There were also told that, inside, there was a free-moving object which could fall randomly into one of the three inner tubes. The subjects had to guess in which inner tube the object fell by **tilting the tube only twice: first tipping downward, then lifting upward**. They had no further instruction nor any feedback, before or during the trials. They reported their answer by pointing to one of the markings on the tube (Figure 6.4). They were instructed to use only shallow angles and were asked to wear sound blocking ear muffs. Each subject performed the task 30 times where each of the three simulated length was presented 10 times in randomized order. Typically they completed the 30 trials within a few minutes. After the trials, they were debriefed and the nature of the apparatus was revealed to them.

6.6 Results

6.6.1 Scores

The total numbers of guesses for each length category are collected in Figure 6.7. For both the impact and the rolling cue, the subjects' guesses for the shortest and medium lengths (18 cm and 24 cm) were very similar. By and large, they were not able to distinguish between them and performed nearly at chance between these two cases. On the other hand, for the longest length (60 cm) they were generally very good at guessing it apart from the medium and shortest ones. The simulation and the cues provided enough information for most subjects.

With only the impact cue available, most subjects chose *medium* for the two short

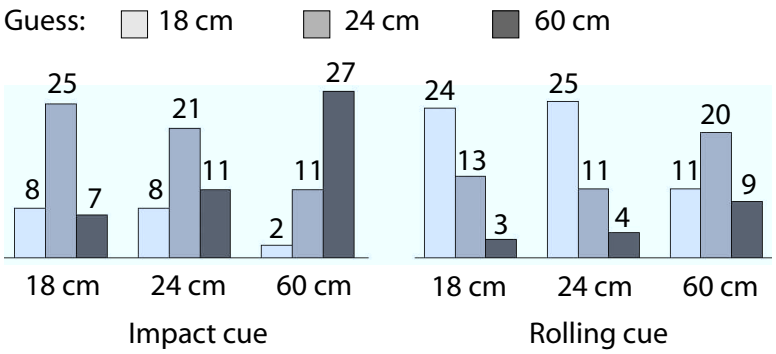

Fig. 6.7 Total number of estimation for each simulated length

cases, and *longest* for the long case. However, when only the rolling cue was available, most subjects chose *shortest* for the two short cases, and *medium* for the long one. This seems to indicate a slight tendency to overestimate length given the impact cue only and a more marked tendency to underestimated the simulated length given the rolling cue only. The subject pool was too small however to be able to collect statistically meaningful results.

In both experimental conditions, because of the absence of training the performance varied greatly among subjects. Some were very consistent and successful at guessing correctly, but some performed nearly at chance. Figure 6.8 and Figure 6.9 give examples of such cases. It is worth mentioning that the two subjects with the worse performance *spontaneously offered* that they were "not good at this" even before starting the trials. The subjects with the best performance, however, represent the general trend very well indeed.

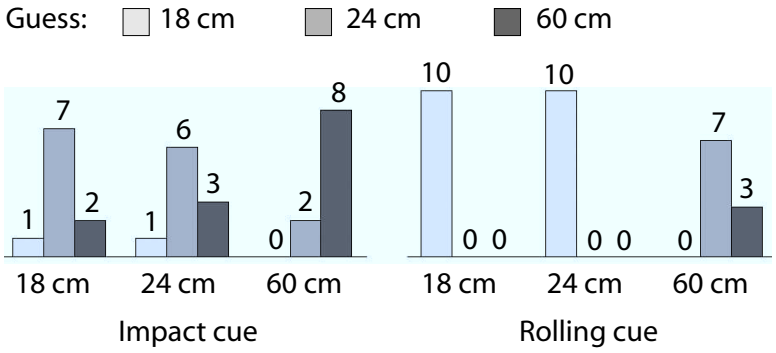

Fig. 6.8 Scores of subjects with best performance.

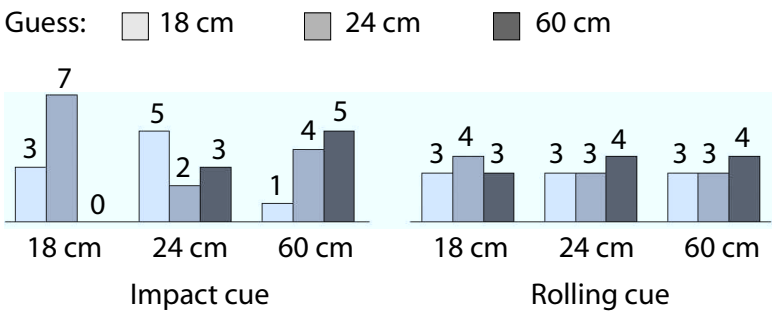

Fig. 6.9 Scores of subjects with worse performance.

6.6.2 Subjective Comments and Observations

The subjects did not know how the sensation of a moving object was created but said that they could visualize the object without problem. In fact, it was quite interesting to observe their typical posture and behavior while attending to the task. Figure 6.10 attempts to capture this. Most remarkably, what subjects appeared to do was to "track" the virtual object with their eyes. This seemed to help them to locate the invisible wall inside the tube, although some noticed that something was "not exactly right."

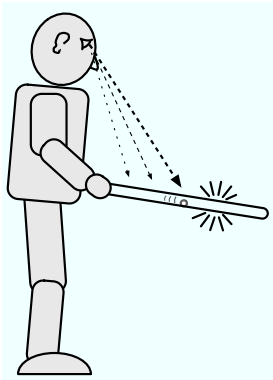

Fig. 6.10 Typical posture during the experiment.

Most subjects agreed that the rolling haptic noise or the haptic impact were realistic. Some were extremely surprised to learn there was no rolling ball inside the tube. When only the impact cue was provided, some subjects commented that since they were unable to feel an object roll, it must have been light, but the impact was strong, creating a conflict. This comment was given once the mechanism of the apparatus was revealed.

After the trials, we also let the subjects experience the rolling noise cue together with

the impact cue. Most felt that this was indeed a lot more realistic, and that having both cues would make the estimation task easier. Some subjects were surprised when they used the apparatus without the impact cue and when it was later turned on. The channel suddenly appeared to be a lot longer.

Most subjects commented about the absence of weight transfer as the virtual ball rolled down the tube. Their comments were different depending on whether they had the impact cue or the rolling cue. Those who received only the impact cue noticed the absence of weight transfer, but those who received only the rolling cue were amazed to find out there was no weight transfer whatsoever. The rolling noise was sufficiently convincing to create the illusion of weight transfer which perhaps is a case of a "pseudo haptic" sensation [148]. In addition, because the experiment required them to tilt the tip first downward and then upward, they tended to use a larger inclination angle when they tilted the tube upwards, as if they tried to compensate for the higher torque due to the mass being at the extremity of the tube in a form of anticipatory movement [149, 143]. Some subjects even reported that the length seemed to be shorter when the ball rolled back (perhaps because of the larger tilt angle), even though the apparatus was well calibrated.

We observed that sometimes the subjects were able to give a definitive answer without hesitation, even after tilting the rod downward only once. Sometimes, however, they seemed confused and took several seconds to make a choice. Some users appeared to hesitate more than others, and this occurred both in the rolling and impact cue conditions.

6.7 Discussion

The results suggest that even with an impoverished sensorimotor coupling, most subjects were able to perform much better than at chance in guessing the size of an inner cavity inside which an object moves under its own dynamics. Given the conditions in which the trials were administered, the results cannot be explained by cognitive factors although this possibility cannot be entirely excluded at this stage. It is conceivable that the subjects might have used the recall of previous trials to discriminate between virtual tube lengths, even if this was difficult to do within a small number of trials. This suggests that the subjects must have had several invariants available to them and that they were able to use them spontaneously, something O'Regan and Noe call the "mastery of patterns of sensorimotor contingency" [93].

We also observed that different haptic cues contributed differently to the task. The results suggest that the impact cue provides the subjects with better estimates around the real value, it is however somewhat ambiguous. With the rolling noise cue the subjects tended to be more consistent, but they under-estimated the distance covered by the virtual object. Estimating the elapsed time *between* two events (roll onset and subsequent impact) seems to be harder to use than estimating the *duration* of one event (rolling noise). It is also possible that subjects also used information related to spectral shift in the rolling cue which was not available for those who experienced the impact cue only.

The large performance gaps from one subject to another is rather interesting. One explanation is the variability in background experience. Without specific training, some people may not be particularly good at, or even unable to, using these cues to judge distances. They may normally rely on cues not made available to them during the experiment, such as weight transfer, acoustic feedback or prior knowledge of the material and inertia of the moving object.

Sufficient realism of the simulation was confirmed by the surprise expressed by most subjects upon debriefing. Although most subjects suspected that there was something unnatural about the apparatus, they had no trouble developing mental imagery associated with a rolling or a sliding object.

6.8 Conclusion

Future experiments could explore additional haptic cues or cues from other modalities, and explore their interactions. With the addition of well designed acoustic cues specifically, more interesting results may be obtained. In [150], the audio synthesis of the sound made by a rolling ball is suggested to be sufficient to enable the creation a new kinds of human computer interfaces. Systems similar to our apparatus may have applications in human-computer interaction and several other areas. For example, in [18], additional haptic feedback in portable devices is said to be useful to functions other than just alerts such as data input. Oackley et al, as well as Linjama et al, have applied the principle of *tilting* a hand-held device and combined it with haptic feedback to devise new human-computer interfaces techniques [151, 152]. In computer music performance, the use of tactile feedback coupled with movement was proposed to aid the execution of gestures in "thin air" [153]. In all these examples, the authors observed that several interesting perceptual effects occurred

for certain sensorimotor couplings which are not unlike that explored in the present paper.

6.9 Acknowledgments

Hsin-Yun Yao would like to thank NSERC, the Natural Sciences and Engineering Council of Canada, for an Industrial Postgraduate Scholarship with complementary support from Immersion Corporation. Vincent Hayward acknowledges the continuing support of NSERC for a Discovery Grant titled "High Fidelity Haptics."

Chapter 7

Conclusion

The challenge of advancing the state of the art in ambient haptic system has two facets: on the one hand, it requires technical advancements in interfaces and devices to transmit information; on the other hand, in order to communicate efficiently using perceptually relevant signals, one needs more understanding about haptic perception. It is by nature a multi-disciplinary task. By approaching the problem from three different aspects, the author aims to make contributions, as presented in the thesis, which are versatile and applicable in different areas in haptics research.

Thesis Summary and Conclusions

Naturally occurring in daily activities, vibrotactile signals play an important role in the degree of realism of haptic event simulation. The goal of this research is to find ways to improve the realism of vibrotactile devices suitable for use in ambient systems. The major lines of inquires in this thesis are the following: the first is the design of a novel vibrotactile transducer, followed by two studies, one on vibration perception and one on haptic perception of the rolling distance, both implemented using the above transducer.

To begin with, the first goal was to improve the state of the art vibrotactile transducers. Despite the great intention and effort put into portable haptic display, there seemed to be some unfilled gaps, especially the lack of simple, reliable and higher quality transducers designed for haptics. Among the possible actuating mechanisms, the voice-coil motors had the potential to deliver higher bandwidth and controllability compared to common vibration DC motors. As electromotive devices manufacturing is well understood, such a

transducer can be manufactured with minimal cost. In Chapter 3, the design, analysis and modeling of a voice-coil vibrotactile transducer was presented. The moving magnet design was chosen because a bigger moving mass can provide a larger force. The frequency response of the transducer showed that it has a bandwidth covering the 50-400 Hz range, optimal for vibrotactile sensation. The system was modeled by converting a mechanical free-diagram to electrical equivalent circuit. The transfer function was first found experimentally, then combined with the theoretical expression to find the unknown suspension term. After the model was obtained, the sensibility of each parameter was analyzed with respect to the output acceleration.

Following the actuator design, Chapter 4 and 5 described a series of experiment studies targeting vibrotactile signals on mobile devices. Prior studies on vibrotactile perception mostly focused on how the vibration strength is related to unpleasantness and health hazards, thereby regarding vibration as background noise that should be suppressed. However, for mobile devices, vibration signals are a sought-after feature, capable of attracting attention in a non-invasive way. Most questions about the attention-grabbing function of vibrating signals are still unanswered. In this study, experiments were carried out to relate the perceived vibration strength with two factors: the device weight and the underlying vibration frequency, in the context of a mobile device. The vibrotactile transducer proposed earlier was the essential component in the fabrication of the experimental apparatuses (mock cellphones). The results suggested that for the same measured acceleration, a heavier weight is perceived to vibrate with a greater strength. For a higher underlying frequency, the same measured acceleration has a weaker perceived strength.

The experiment detailed in Chapter 6 served as a pertinent example of how the aforementioned actuator could be used in an ambient haptic system. The haptic device developed for this particular study was a hollow rod equipped with an inclination sensor and the aforementioned vibrotactile actuator. It was capable of simulating realistic vibrotactile signals that arise when a ball is rolled down a tube and encounters an inner stop. During the experiment, participants were asked to hold, tilt the rod, feel the inside ball rolling, and estimate how far the ball had rolled using a haptic signal only. The results confirmed that one could provide a rough estimate of the traveled distance. By decomposing the cues into rolling signals and impact signals, we found that rolling cues provide a more accurate estimation of the rolling distance.

In conclusion, Chapter 3 showed that a voice-coil vibrotactile transducer is capable of

improving the signal bandwidth under the enclosure vibration paradigm. Although not a comprehensive study of vibrotactile perception on mobile devices, Chapter 5 contributed to a better understanding and attempted to raise awareness about a lack of research-based industry guidelines on vibrotactile communication. The importance of the contribution detailed in Chapter 6 stems from the fact that the experiment was based on a haptic modality instead of visual modality, suggesting that the gravity model is accessible across different modalities.

Future Work

A follow-up study of the rolling stone experiment has been carried out in collaboration with Ilja Frisson, the principle investigator. Results of experiments on rolling distance estimation using real and simulated balls further supported our previous finding. This study is now complete and in the process of manuscript preparation. One direction of future work is to look into the auditory modality and to examine closer the process of sensory integration in this task. Another direction is to probe further on why we tend to visually track the invisible rolling ball even though the necessary information is only present in the haptic domain.

The vibrotactile transducer proposed in this thesis has the potential to be manufactured for a reasonable cost. It is also possible to be fabricated in different sizes and dimensions to suit different applications. In particular, it would be suitable for perception studies specific to mobile devices, such as the frequency of the pulsing scheme or the attention grabbing ability of different signals. It can also be used to provide enriched portable vibrotactile display for virtual-reality studies, similar to the "Shoogle" [38], or for studies on haptic or tactile icons. One important step is to make it widely available for a broader research community to benefit from it, and to suggest ideas on possible improvement in the future.

References

[1] A. Al Mamun, G. Guo, and C. Bi, *Hard disk drive: mechatronics and control*. CRC, 2006.

[2] K. Kim, S. Lee, and S. Kim, "A mobile auto-focus actuator based on a rotary VCM with the zero holding current," *Optics Express*, vol. 17, no. 7, pp. 5891–5896, 2009.

[3] N. Bianchi, S. Bolognani, D. D. Corte, and F. Tonel, "Tubular linear permanent magnet motors: an overall comparison," *IEEE Transactions on Industry Applications*, vol. 39, no. 2, pp. 466–475, 2003.

[4] M. B. Khoudja, M. Hafez, J.-M. Alexandre, and A. Kheddar, "Tactile interfaces: a state of the art survey," in *International Symposium on Robotics*, (Paris), March 2004.

[5] L. A. Jones and D. A. Held, "Characterization of tactors used in vibrotactile displays," *Journal of Computing and Information Science in Engineering*, vol. 8, no. 4, p. 044501, 2008.

[6] K. Tsukada and M. Yasumura, "Activebelt: Belt-type wearable tactile display for directional navigation," *Lecture Notes in Computer Science*, vol. 3205, pp. 384–399, 2004.

[7] F. Gemperle, N. Ota, and D. Siewiorek, "Design of a wearable tactile display," in *Wearable Computers, 2001. Proceedings. Fifth International Symposium on*, pp. 5–12, 2001.

[8] Y. Yanagida, M. Kakita, R. Lindeman, Y. Kume, and N. Tetsutani, "Vibrotactile letter reading using a low-resolution tactor array," in *Haptic Interfaces for Virtual Environment and Teleoperator Systems, 2004. HAPTICS'04. Proceedings. 12th International Symposium on*, pp. 400–406, 2004.

[9] A. Chang, S. O'Modhrain, R. Jacob, E. Gunther, and H. Ishii, "ComTouch: design of a vibrotactile communication device," in *Proceedings of the 4th conference on Designing interactive systems: processes, practices, methods, and techniques*, pp. 312–320, ACM New York, NY, USA, 2002.

[10] M. Niwa, Y. Yanagida, H. Noma, K. Hosaka, and Y. Kume, "Vibrotactile apparent movement by DC motors and voice-coil tactors," in *Proceedings of The 14th International Conference on Artificial Reality and Telexistence (ICAT), Seoul, Korea*, pp. 126–131, 2004.

[11] D. A. Kontarinis and R. D. Howe, "Tactile display of vibratory information in teleoperation and virtual environments.," *Presence: Teleoperators and Virtual Environments*, vol. 4, no. 4, pp. 387–402, 1995.

[12] A. Okamura, M. Cutkosky, and J. Dennerlein, "Reality-based models for vibration feedback in virtual environments," *IEEE/ASME Transactions on Mechatronics*, vol. 6, no. 3, pp. 245–252, 2001.

[13] M. Marshall and M. Wanderley, "Vibrotactile feedback in digital musical instruments," in *Proceedings of the 2006 conference on New interfaces for musical expression*, pp. 226–229, IRCAM—Centre Pompidou Paris, France, France, 2006.

[14] L. Kohli, M. Niwa, H. Noma, K. Susami, Y. Yanagida, R. Lindeman, K. Hosaka, and Y. Kume, "Towards Effective Information Display Using Vibrotactile Apparent Motion," in *Haptic Interfaces for Virtual Environment and Teleoperator Systems, 2006 14th Symposium on*, pp. 445–451, 2006.

[15] B. J. Mortimer, G. A. Zets, and R. W. Cholewiak, "Vibrotactile transduction and transducers.," *The Journal of the Acoustical Society of America*, vol. 121, no. 5 Pt1, p. 2970, 2007.

[16] L. Brown, S. Brewster, and H. Purchase, "A first investigation into the effectiveness of tactons," in *Proc. World Haptics*, pp. 167–176, 2005.

[17] J. Hijmans, J. Geertzen, B. Schokker, and K. Postema, "Development of vibrating insoles," *International Journal of Rehabilitation Research*, vol. 30, no. 4, p. 343, 2007.

[18] I. Poupyrev, S. Maruyama, and J. Rekimoto, "Ambient touch: Designing tactile interfaces for handheld devices touch: Designing tactile interfaces for handheld devices," in *ACM UIST*, pp. 51–60, 2002.

[19] I. Poupyrev, J. Rekimoto, and S. Maruyama, "TouchEngine: a tactile display for handheld devices," in *Conference on Human Factors in Computing Systems*, pp. 644–645, ACM New York, NY, USA, 2002.

[20] H. Kajimoto, N. Kawakami, S. Tachi, and M. Inami, "SmartTouch: Electric skin to touch the untouchable," *IEEE Computer Graphics and Applications*, vol. 24, no. 1, pp. 36–43, 2004.

[21] A. Yamamoto, T. Ishii, and T. Higuchi, "Electrostatic tactile display for presenting surface roughness sensation," in *2003 IEEE International Conference on Industrial Technology*, vol. 2, 2003.

[22] P. Wellman, W. Peine, G. Favalora, and R. Howe, "Mechanical design and control of a high-bandwidth shape memory alloy tactile display," in *Experimental Robotics V, Lecture Notes in Control and Information Science 232,* (A. Casals and A. T. de Almeida, eds.), pp. 56–66, Springer Verlag, 1998.

[23] C. Wagner, S. Lederman, and R. Howe, "Design and performance of a tactile shape display using RC servomotors," *Haptics-e*, vol. 3, no. 4, 2004.

[24] Y. Ikei, K. Wakamatsu, and S. Fukuda, "Vibratory tactile display of image-based textures," *IEEE Computer Graphics and Applications*, vol. 17, no. 6, pp. 53–61, 1997.

[25] M. Benali-Khoudja, M. Hafez, J. Alexandre, A. Kheddar, and V. Moreau, "VITAL: a new low-cost vibro-tactile display system," in *Robotics and Automation, 2004. Proceedings. ICRA'04. 2004 IEEE International Conference on*, vol. 1, 2004.

[26] V. Hayward and M. Cruz-Hernandez, "Tactile display device using distributed lateral skin stretch," in *Proc. of the Haptic Interfaces for Virtual Environment and Teleoperator Systems Symposium (IMECE2000)*, vol. DSC-69-2, pp. 1309–1314, ASME, 2000.

[27] Q. Wang, V. Levesque, J. Pasquero, and V. Hayward, "A haptic memory game using the STRESS 2 tactile display," in *Conference on Human Factors in Computing Systems*, pp. 271–274, ACM New York, NY, USA, 2006.

[28] V. Levesque and V. Hayward, "Experimental evidence of lateral skin strain during tactile exploration," in *Proc. Eurohaptics 2003*, pp. 261–275, 2003.

[29] T. Kaaresoja and J. Linjama, "Perception of Short Tactile Pulses Generated by a Vibration Motor in a Mobile Phone," in *Proceedings of First Joint EuroHaptics Conference and Symposium on Haptic Interfaces for Virtual Environment and Teleoperator Systems*, pp. 471–472, 2005.

[30] S. Töyssy, "Telling Time by Vibration," *Department of Computer Sciences, University of Tampere, Master's Thesis, November*, 2007.

[31] S. Kim and K. Kim, "Interactive Racing Game with Graphic and Haptic Feedback," *Lecture Notes in Computer Science*, vol. 4813, p. 69, 2007.

[32] L. Brown and T. Kaaresoja, "Feel who's talking: using tactons for mobile phone alerts," in *Conference on Human Factors in Computing Systems*, pp. 604–609, ACM New York, NY, USA, 2006.

[33] J. Jung and S. Choi, "Perceived magnitude and power consumption of vibration feedback in mobile devices," in *HCI (2)*, pp. 354–363, 2007.

[34] J. Ryu and S. Choi, "Benefits of perceptually transparent vibration rendering in mobile device," in *Proceedings of EuroHaptics 2008*, pp. 706–711, 2008.

[35] J. Ryu, J. Jung, S. Kim, and S. Choi, "Perceptually transparent vibration rendering using a vibration motor for haptic interaction," *Robot and Human interactive Communication, The 16th IEEE International Symposium on*, pp. 310–315, Aug. 2007.

[36] J. Ryu, J. Jung, and S. Choi, "Perceived magnitudes of vibrations transmitted through mobile device," *11th Symposium on Haptic Interfaces for Virtual Environment and Teleoperator Systems Proceedings*, pp. 139–140, March 2008.

[37] J. Linjama and T. Kaaresoja, "Novel, minimalist haptic gesture interaction for mobile devices," in *Proceedings of the third Nordic conference on Human-computer interaction*, pp. 457–458, ACM New York, NY, USA, 2004.

[38] J. Williamson, R. Murray-Smith, and S. Hughes, "Shoogle: excitatory multimodal interaction on mobile devices," in *Proceedings of the SIGCHI conference on Human factors in computing systems*, pp. 121–124, ACM New York, NY, USA, 2007.

[39] A. Okamura, J. Dennerlein, and R. Howe, "Vibration feedback models for virtual environments," in *1998 IEEE International Conference on Robotics and Automation, 1998. Proceedings*, vol. 1, 1998.

[40] M. Srinivasan and C. Basdogan, "Haptics in virtual environments: Taxonomy, research status, and challenges," *Computers & Graphics*, vol. 21, no. 4, pp. 393–404, 1997.

[41] Y. Ikei and M. Shiratori, "TextureExplorer: A tactile and force display for virtual textures," in *Haptic Interfaces for Virtual Environment and Teleoperator Systems, 2002. HAPTICS 2002. Proceedings. 10th Symposium on*, pp. 327–334, 2002.

[42] G. Campion and V. Hayward, "Fundamental limits in the rendering of virtual haptic textures," in *Proceedings of the First Joint Eurohaptics Conference and Symposium on Haptic Interfaces for Virtual Environment and Teleoperator Systems, World Haptics*, vol. 2005, pp. 263–270, 2005.

[43] S. Choi and H. Tan, "Toward realistic haptic rendering of surface textures," in *International Conference on Computer Graphics and Interactive Techniques*, ACM New York, NY, USA, 2005.

[44] I. Poupyrev, M. Okabe, and S. Maruyama, "Haptic feedback for pen computing: directions and strategies," in *Conference on Human Factors in Computing Systems*, pp. 1309–1312, ACM New York, NY, USA, 2004.

[45] J. Lee, P. Dietz, D. Leigh, W. Yerazunis, and S. Hudson, "Haptic pen: a tactile feedback stylus for touch screens," in *Symposium on User Interface Software and Technology: Proceedings of the 17 th annual ACM symposium on User interface software and technology*, Association for Computing Machinery, Inc, One Astor Plaza, 1515 Broadway, New York, NY, 10036-5701, USA,, 2004.

[46] C. Liao, F. Guimbretière, and C. Loeckenhoff, "Pen-top feedback for paper-based interfaces," in *Proceedings of the 19th annual ACM symposium on User interface software and technology*, pp. 201–210, ACM New York, NY, USA, 2006.

[47] H. Yao, V. Hayward, and R. Ellis, "A tactile enhancement instrument for minimally invasive surgery," *Computer Aided Surgery*, vol. 10, no. 4, pp. 233–239, 2005.

[48] H. Yao and V. Hayward, "A Network-ready Multi-lateral High Fidelity Haptic Probe," in *Haptic Interfaces for Virtual Environment and Teleoperator Systems, 2006 14th Symposium on*, pp. 81–82, 2006.

[49] M. Bovenzi, "Exposure-response relationship in the hand-arm vibration syndrome: an overview of current epidemiology research," *International archives of occupational and environmental health*, vol. 71, no. 8, pp. 509–519, 1998.

[50] K. Johnson, "The roles and functions of cutaneous mechanoreceptors," *Current Opinion in Neurobiology*, vol. 11, no. 4, pp. 455–461, 2001.

[51] F. Konietzny and H. Hensel, "Response of rapidly and slowly adapting mechanoreceptors and vibratory sensitivity in human hairy skin," *Pflügers Archiv European Journal of Physiology*, vol. 368, no. 1, pp. 39–44, 1977.

[52] R. Verrillo, "Investigation of some parameters of the cutaneous threshold for vibration," *The Journal of the Acoustical Society of America*, vol. 34, p. 1768, 1962.

[53] D. Reynolds, K. Standlee, and E. Angevine, "Hand-arm vibration, Part III: Subjective response characteristics of individuals to hand-induced vibration," *Journal of Sound and Vibration*, vol. 51, no. 2, pp. 267–282, 1977.

[54] T. Miwa, "Evaluation Methods for Vibration Effect: Part 3. Measurements of Threshold and Equal Sensation Contours on Hand for Vertical and Horizontal Sinusoidal Vibrations," *Industrial Health*, vol. 5, pp. 213–220, 1967.

[55] N. Harada and M. Griffin, "Factors influencing vibration sense thresholds used to assess occupational exposures to hand transmitted vibration.," *British Medical Journal*, vol. 48, no. 3, p. 185, 1991.

[56] R. Verrillo, "Effect of contact area on the vibrotactile threshold," *Journal of the Acoustical Society of America*, vol. 35, pp. 1962–1966, 1963.

[57] M. Morioka and M. Griffin, "Equivalent comfort contours for vertical vibration of steering wheels: Effect of vibration magnitude, grip force, and hand position," *Applied Ergonomics*, 2008.

[58] P. Lamore and C. Keemink, "Evidence for different types of mechanoreceptors from measurements of the psychophysical threshold for vibrations under different stimulation conditions," *The Journal of the Acoustical Society of America*, vol. 83, p. 2339, 1988.

[59] M. Morioka and M. Griffin, "Magnitude-dependence of equivalent comfort contours for fore-and-aft, lateral and vertical hand-transmitted vibration," *Journal of Sound and Vibration*, vol. 295, no. 3-5, pp. 633–648, 2006.

[60] G. Gescheider, S. Bolanowski, K. Hall, K. Hoffman, and R. Verrillo, "The effects of aging on information-processing channels in the sense of touch: I. Absolute sensitivity," *Somatosensory and Motor Research*, vol. 11, no. 4, pp. 345–357, 1994.

[61] P. Willes, S. Pearce, P. Rice, and J. Mitchell, "Vibration perception threshold: influence of age, height, sex, and smoking, and calculation of accurate centile values," *Diabetic medicine*, vol. 8, no. 2, pp. 157–161, 1991.

[62] P. Halonen, "Quantitative vibration perception thresholds in healthy subjects of working age," *European Journal of Applied Physiology*, vol. 54, no. 6, pp. 647–655, 1986.

[63] S. Bolanowski, G. Gescheider, and R. Verrillo, "Hairy skin: psychophysical channels and their physiological substrates," *Somatosensory and Motor Research*, vol. 11, no. 3, pp. 279–290, 1994.

[64] S. Stevens, "Tactile vibration: Dynamics of sensory intensity," *Journal of Experimental Psychology*, vol. 57, no. 4, pp. 210–218, 1959.

[65] R. Verrillo, A. Fraioli, and R. Smith, "Sensation magnitude of vibrotactile stimuli," *Perception & Psychophysics*, vol. 6, no. 6, pp. 366–372, 1969.

[66] J. Giacomin, M. Shayaa, E. Dormegnie, and L. Richard, "Frequency weighting for the evaluation of steering wheel rotational vibration," *International Journal of Industrial Ergonomics*, vol. 33, no. 6, pp. 527–541, 2004.

[67] A. Brisben, S. Hsiao, and K. Johnson, "Detection of Vibration Transmitted Through an Object Grasped in the Hand," *Journal of Neurophysiology*, vol. 81, no. 4, pp. 1548–1558, 1999.

[68] M. Morioka and M. Griffin, "Thresholds for the perception of hand-transmitted vibration: Dependence on contact area and contact location," *Somatosensory and Motor Research*, vol. 22, no. 4, pp. 281–297, 2005.

[69] S. Amman, R. Meier, K. Trost, and P. Gu, "Equal Annoyance Contours for Steering Wheel Hand-Arm Vibration," 2005.

[70] D. Mahns, N. Perkins, V. Sahai, L. Robinson, and M. Rowe, "Vibrotactile Frequency Discrimination in Human Hairy Skin," *Journal of Neurophysiology*, vol. 95, no. 3, pp. 1442–1450, 2006.

[71] M. Tommerdahl, K. Hester, E. Felix, M. Hollins, O. Favorov, P. Quibrera, and B. Whitsel, "Human vibrotactile frequency discriminative capacity after adaptation to 25 Hz or 200 Hz stimulation," *Brain Research*, vol. 1057, no. 1-2, pp. 1–9, 2005.

[72] S. Bensmaïa and M. Hollins, "Complex tactile waveform discrimination," *The Journal of the Acoustical Society of America*, vol. 108, p. 1236, 2000.

[73] G. Gescheider, S. Bolanowski Jr, R. Verrillo, D. Arpajian, and T. Ryan, "Vibrotactile intensity discrimination measured by three methods," *The Journal of the Acoustical Society of America*, vol. 87, p. 330, 1990.

[74] R. Verrillo and G. Gescheider, "Effect of prior stimulation on vibrotactile thresholds.," *Sensory processes*, vol. 1, no. 4, p. 292, 1977.

[75] K. Nishiyama and S. Watanabe, "Temporary threshold shift of vibratory sensation after clasping a vibrating handle," *International Archives of Occupational and Environmental Health*, vol. 49, no. 1, pp. 21–33, 1981.

[76] R. Lundström and R. Johansson, "Acute impairment of the sensitivity of skin mechanoreceptive units caused by vibration exposure of the hand," *Ergonomics*, vol. 29, no. 5, pp. 687–698, 1986.

[77] S. O'Mara, M. Rowe, and R. Tarvin, "Neural mechanisms in vibrotactile adaptation," *Journal of neurophysiology*, vol. 59, no. 2, pp. 607–622, 1988.

[78] G. Lundborg, C. Sollerman, T. Stromberg, I. Pyykko, and B. Rosén, "A new principle for assessing vibrotactile sense in vibration-induced neuropathy.," *Scandinavian journal of work, environment & health*, vol. 13, no. 4, p. 375, 1987.

[79] L. Krueger, "1. Tactual perception in historical perspective: David Katz's world of touch," *Tactual perception: A sourcebook*, p. 1, 1982.

[80] M. Taylor and S. Lederman, "Tactile roughness of grooved surfaces: A model and the effect of friction," *Perception & Psychophysics*, vol. 17, no. 1, pp. 23–36, 1975.

[81] C. Cascio and K. Sathian, "Temporal cues contribute to tactile perception of roughness," *Journal of Neuroscience*, vol. 21, no. 14, p. 5289, 2001.

[82] M. Hollins, S. Bensmaïa, and S. Washburn, "Vibrotactile adaptation impairs discrimination of fine, but not coarse, textures," *Somatosensory and Motor Research*, vol. 18, no. 4, pp. 253–262, 2001.

[83] M. Hollins, S. Bensmaïa, and E. Roy, "Vibrotaction and texture perception," *Behavioural brain research*, vol. 135, no. 1-2, pp. 51–56, 2002.

[84] E. Gamzu and E. Ahissar, "Importance of temporal cues for tactile spatial-frequency discrimination," *Journal of Neuroscience*, vol. 21, no. 18, p. 7416, 2001.

[85] M. Hollins, R. Faldowski, S. Rao, and F. Young, "Perceptual dimensions of tactile surface texture: A multidimensional scaling analysis," *Perception and Psychophysics*, vol. 54, no. 6, pp. 697–705, 1993.

[86] D. Picard, C. Dacremont, D. Valentin, and A. Giboreau, "Perceptual dimensions of tactile textures," *Acta psychologica*, vol. 114, no. 2, pp. 165–184, 2003.

[87] R. Klatzky and S. Lederman, "Tactile roughness perception with a rigid link interposed between skin and surface," *Perception and Psychophysics*, vol. 61, no. 4, pp. 591–607, 1999.

[88] R. Klatzky, S. Lederman, C. Hamilton, M. Grindley, and R. Swendsen, "Feeling textures through a probe: Effects of probe and surface geometry and exploratory factors," *Perception and Psychophysics*, vol. 65, no. 4, pp. 613–631, 2003.

[89] T. Yoshioka, S. Bensmaïa, J. Craig, and S. Hsiao, "Texture perception through direct and indirect touch: An analysis of perceptual space for tactile textures in two modes of exploration," *Somatosensory and Motor Research*, vol. 24, no. 1, pp. 53–70, 2007.

[90] K. Kuchenbecker, J. Fiene, and G. Niemeyer, "Improving contact realism through event-based haptic feedback," *IEEE Transactions on Visualization and Computer Graphics*, vol. 12, no. 2, pp. 219–230, 2006.

[91] J. Sreng, A. Lecuyer, and C. Andriot, "Using vibration patterns to provide impact position information in haptic manipulation of virtual objects," *LECTURE NOTES IN COMPUTER SCIENCE*, vol. 5024, p. 589, 2008.

[92] R. Cross, "The sweet spot of a baseball bat," *American Journal of Physics*, vol. 66, no. 9, pp. 772–778, 1998.

[93] J. K. O'Regan and A. Noe, "A sensorimotor account of vision and visual consciousness," *Behavioral And Brain Sciences*, vol. 24, no. 5, 2001.

[94] M. Mossio and D. Taraborelli, "Action-dependent perceptual invariants: From ecological to sensorimotor approaches," *Consciousness and Cognition*, vol. 17, no. 4, pp. 1324–1340, 2008.

[95] D. Wolpert, Z. Ghahramani, and M. Jordan, "An internal model for sensorimotor integration," *Science*, vol. 269, no. 5232, pp. 1880–1882, 1995.

[96] D. Merfeld, L. Zupan, and R. Peterka, "Humans use internal models to estimate gravity and linear acceleration," *Nature*, vol. 398, no. 6728, pp. 615–618, 1999.

[97] I. Kim and E. Spelke, "Infants'sensitivity to effects of gravity on visible object motion.," *Journal of experimental psychology. Human perception and performance*, vol. 18, no. 2, p. 385, 1992.

[98] M. Zago and F. Lacquaniti, "Visual perception and interception of falling objects: A review of evidence for an internal model of gravity," *Journal of Neural Engineering*, vol. 2, no. 3, pp. S198–S208, 2005.

[99] M. Zago, J. McIntyre, P. Senot, and F. Lacquaniti, "Visuo-motor coordination and internal models for object interception," *Experimental Brain Research*, vol. 192, no. 4, pp. 571–604, 2009.

[100] M. Zago and F. Lacquaniti, "Internal model of gravity for hand interception: parametric adaptation to zero-gravity visual targets on Earth," *Journal of Neurophysiology*, vol. 94, no. 2, pp. 1346–1357, 2005.

[101] J. McIntyre, M. Zago, A. Berthoz, and F. Lacquantini, "Does the brain model Newton's laws?," *Nature Neuroscience*, vol. 4, no. 7, pp. 693–694, 2001.

[102] I. Indovina, V. Maffei, G. Bosco, M. Zago, E. Macaluso, and F. Lacquaniti, "Representation of visual gravitational motion in the human vestibular cortex," 2005.

[103] F. Lacquaniti and C. Maioli, "Adaptation to suppression of visual information during catching," *Journal of Neuroscience*, vol. 9, no. 1, pp. 149–159, 1989.

[104] K. E. MacLean, *Haptic Interaction Design for Everyday Interfaces*, pp. 149–194. Santa Monica, California, USA: Human Factors and Ergonomics Society, 2008.

[105] L. A. Jones and N. B. Sarter, "Tactile displays: Guidance for their design and application," *Human Factors: The Journal of the Human Factors and Ergonomics Society*, vol. 50, no. 1, pp. 90–111, 2008.

[106] R. H. Gault, "Recent developments in vibro-tactile research," *Journal of the Franklin Institute*, vol. 221, pp. 703–719, 1936.

[107] S.-U. Chung, G.-Y. Hwang, S.-M. Hwang, B.-S. Kang, and H.-G. Kim, "Development of brushless and sensorless vibration motor used for mobile phone," *IEEE Transactions on Magnetics*, vol. 38, no. 5, pp. 3000–3002, 2002.

[108] H.-Y. Yao, D. Grant, and M. Cruz-Hernandez, "Perceived vibration strength in mobile devices: the effect of weight and frequency," *IEEE Transaction on Haptics*, vol. in press, 2009.

[109] D. Bailey, D. Grant, A. Jasso, E. Shahoin, K. Tierling, and S. Vassallo, *Haptic feedback using rotary harmonic moving mass.* US Patent 7,161,580, Jan. 9 2007.

[110] V. Hayward and K. E. MacLean, "Do it yourself haptics, part-i," *IEEE Robotics and Automation Magazine*, vol. 14, no. 4, pp. 88–104, 2007.

[111] R. E. Clark, G. W. Jewell, and D. Howe, "Dynamic modeling of tubular moving-magnet linear actuators," *Journal of Applied Physics*, vol. 93, no. 10, pp. 8787–8789, 2003.

[112] L. N. Tutelea, M. C. Kim, M. Topor, J. Lee, and I. Boldea, "Linear permanent magnet oscillatory machine: Comprehensive modeling for transients with validation by experiments," *IEEE Transactions on Industrial Electronics*, vol. 55, no. 2, pp. 492–500, 2008.

[113] D. de Bhailís, C. Murray, M. Duffy, J. Alderman, G. Kelly, and S. C. Ò Mathúna, "Modelling and analysis of a magnetic microactuator," *Sensors & Actuators: A. Physical*, vol. 81, no. 1-3, pp. 285–289, 2000.

[114] D. Niarchos, "Magnetic MEMS: key issues and some applications," *Sensors & Actuators: A. Physical*, vol. 109, no. 1-2, pp. 166–173, 2003.

[115] J. Wang, D. Howe, and G. Jewell, "Analysis and design optimization of an improved axially magnetized tubular permanent-magnet machine," *IEEE Transaction on Energy Conversion*, vol. 19, no. 2, pp. 289–295, 2004.

[116] S. M. Jang, J. Y. Choi, S. H. Lee, H. W. Cho, and W. B. Jang, "Analysis and experimental verification of moving-magnet linear actuator with cylindrical Halbach array," *IEEE Transactions on Magnetics*, vol. 40, no. 4 Part 2, pp. 2068–2070, 2004.

[117] M. Cruz-Hernandez, D. Grant, and V. Hayward, *Haptic devices having multiple operational modes including at least one resonant mode.* US Patent 7,369,115, May 6 2008.

[118] I. Poupyrev and S. Maruyama, "Tactile interfaces for small touch screens," in *Proceedings of the 13th annual ACM symposium on User interface software and technology (UIST '03)*, vol. 5, pp. 217–220, 2003.

[119] H.-Y. Yao and V. Hayward, "An experiment on length perception with a virtual rolling stone," in *Proceedings of Eurohaptics*, pp. 325–330, 2006.

[120] W. M. Leach, "Loudspeaker voice-coil inductance losses: circuit models, parameter estimation, and effect on frequency response," *Journal of Audio Engineering Society*, vol. 50, no. 6, pp. 442–450, 2002.

[121] C. Alexander and M. Sadiku, *Fundamentals of electric circuits.* New York: McGraw-Hill, 2004.

[122] J. Eargle, *Loudspeaker handbook.* Heidelberg: Springer, 2003.

[123] J. Miles, "Applications and limitations of mechanical-electrical analogies," *Journal of the Acoustical Society of America*, vol. 14, no. 3, pp. 183–192, 1943.

[124] A. Champagne, "Correlation of electric power steering vibration to subjective ratings," 2000.

[125] D. Fleming and M. Griffin, "A study of the subjective equivalence of noise and whole-body vibration," *Journal of Sound and Vibration*, vol. 42, pp. 453–461, 1975.

[126] S. Maeda, "Necessary research for standardization of subjective scaling of whole-body vibration," *Industrial health*, vol. 43, no. 3, pp. 390–401, 2005.

[127] J. Craig and C. Sherrick, "The role of skin coupling in the determination of vibrotactile spatial summation," *Perception & Psychophysics*, vol. 6, pp. 97–101, 1969.

[128] A. Charpentier, "Analyse experimentale de quelques elements de la sensation de poids," *Archives de Physiologie Normales et Pathologiques*, vol. 3, pp. 122–35, 1891.

[129] N. Mansfield and S. Maeda, "Equal sensation curves for whole-body vibration expressed as a function of driving force," *The Journal of the Acoustical Society of America*, vol. 117, p. 3853, 2005.

[130] J. Giacomin and C. Onesti, "Effect of Frequency and grip force on the perception of steering wheel rotational vibration," in *Conference on the New Role of Experimentation in the Modern Automotive Product Development Process, Firenze, Italy*, pp. 17–19, November 1999.

[131] E. H. Weber, *The sense of touch.* (H. E. Ross and D. J. Murray, trans.), Academic Press, 1978 (Original work published 1834).

[132] R. Ellis and S. Lederman, "The role of haptic versus visual volume cues in the size-weight illusion," *Perception & psychophysics*, vol. 53, no. 3, pp. 315–324, 1993.

[133] J. Flanagan and M. Beltzner, "Independence of perceptual and sensorimotor predictions in the size- weight illusion," *Nature Neuroscience*, vol. 3, pp. 737–741, 2000.

[134] M. O. Ernst, "Perceptual learning: Inverting the size–weight illusion," *Current Biology*, vol. 19, no. 1, pp. R23–R25, 2009.

[135] K. Minamizawa, S. Fukamachi, H. Kajimoto, N. Kawakami, and S. Tachi, "Gravity grabber: wearable haptic display to present virtual mass sensation," in *International Conference on Computer Graphics and Interactive Techniques*, ACM Press New York, NY, USA, 2007.

[136] G. Inaba and K. Fujita, "A Pseudo-Force-Feedback Device by Fingertip Tightening for Multi-Finger Object Manipulation," in *Proceedings of EuroHaptics 2006*, pp. 275–278, 2006.

[137] T. Amemiya and T. Maeda, "Asymmetric Oscillation Distorts the Perceived Heaviness of Handheld Objects," *IEEE Transactions on Haptics*, vol. 17, 2008.

[138] H. Yao, V. Hayward, M. Cruz, and D. Grant, "The Effect of Weight on the Perception of Vibrotactile Intensity with Handheld Devices," in *Proceedings of Second Joint EuroHaptics Conference and Symposium on Haptic Interfaces for Virtual Environment and Teleoperator Systems*, pp. 551–552, 2007.

[139] Y. Y. Leung, S. J. Bensmaia, S. S. Hsiao, and K. O. Johnson, "Time-course of vibratory adaptation and recovery in cutaneous mechanoreceptive afferents," *Journal of Neurophysiology*, vol. 94, no. 5, pp. 3037–3045, 2005.

[140] S. J. Bensmaïa, Y. Y. Leung, S. S. Hsiao, and K. O. Johnson, "Vibratory adaptation of cutaneous mechanoreceptive afferents," *Journal of Neurophysiology*, vol. 94, pp. 3023–3036, 2005.

[141] L. Burström and R. Lundström, "Absorption of vibration energy in the human hand and arm," *Ergonomics*, vol. 37, no. 5, pp. 879–890, 1994.

[142] V. Hayward, "Haptic shape cues, invariants, priors, and interface design," in *Human Haptic Perception – Basics and Applications* (M. Grunwald, ed.), ch. 31, pp. 381–392, Birkhauser Verlag, 2008.

[143] P. Senot, M. Zago, F. Lacquaniti, and J. McIntyre, "Anticipating the effects of gravity when intercepting moving objects: Differentiating up and down based on nonvisual cues," *Journal of Neurophysiology*, vol. 94, pp. 4471–4480, 2005.

[144] C. Lenay, S. Canu, and P. Villon, "Technology and perception: The contribution of sensory substitution systems," in *2nd International Conference on Cognitive Technology*, pp. 44–53, 1997.

[145] D. Philipona, J. K. O'Regan, and J.-P. Nadal, "Is there something out there? inferring space from sensorimotor dependencies," *Neural Computation*, vol. 15, no. 9, pp. 2029–2049, 2003.

[146] D. Philipona, J. K. O'Regan, J.-P. Nadal, and O. J.-M. D. Coenen, "Perception of the structure of the physical world using unknown multimodal sensors and effectors," in *Advances in Neural Information Processing Systems*, vol. 16, pp. 945–953, MIT Press, 2004.

[147] G. Robles-De-La-Torre and R. Sekuler, "Numerically estimating internal models of dynamic virtual objects," *ACM Transactions on Applied Perception*, vol. 1, no. 2, pp. 102–117, 2004.

[148] A. Lécuyer, J. Burkhardt, and L. Etienne, "Feeling bumps and holes without a haptic interface: the perception of pseudo-haptic textures," in *Proceedings of the SIGCHI conference on Human factors in computing systems*, pp. 239–246, ACM New York, NY, USA, 2004.

[149] J. Flanagan and A. Wing, "The role of internal models in motion planning and control: evidence from grip force adjustments during movements of hand-held loads," *Journal of Neuroscience*, vol. 17, no. 4, pp. 1519–1528, 1997.

[150] M. Rath and D. Rocchesso, "Continuous sonic feedback from a rolling ball," *IEEE MultiMedia*, vol. 12, no. 2, pp. 60–69, 2005.

[151] I. Oakley, J. Angesleva, S. Hughes, and S. O'Modhrain, "Tilt and feel: Scrolling with vibrotactile display," *EuroHaptics 2004*, 2004.

[152] J. Linjama, J. Hakkila, and S. Ronkainen, "Hands on haptics: Exploring non-visual visualisation using the sense of touch," in *CHI 2005 Workshop on Hands on Haptics: Exploring Non-Visual Visualisation Using the Sense of Touch*, April 2005.

[153] J. Rovan and V. Hayward, "Typology of tactile sounds and their synthesis in gesture-driven computer music performance," in *Trends in Gestural Control of Music*, pp. 297–320, IRCAM, 2000.